Astrocyte-like glia-specific gene *deathstar* is crucial for normal development, adult locomotion and lifespan of male *Drosophila*

Hadi Najafi[1], Kyle Wong[1], Ammar Salkini[1], Hongyu Miao[2], and Woo Jae Kim [1,2,*]

[1]Department of Cellular and Molecular Medicine, Faculty of Medicine, University of Ottawa, Ottawa, Ontario K1H 8M5, Canada

[2]The HIT Center for Life Sciences, Harbin Institute of Technology, Harbin, China.

*Correspondence to: wkim@hit.edu.cn

HN: h.najafi2999@gmail.com KW: kwong132@uottawa.ca AS: asalk017@uottawa.ca HM: 20210125l@stu.hit.edu.cn

ABSTRACT

The nervous system of *Drosophila* is composed of diverse cell types with substantial homologies to various cell types of more complex species, including the human. Among all nervous system cell types, astrocyte-like glia (ALG) is necessary for the proper physiology and behavior of the fly and human. In this study, we exploited the gene expression profile of single cells in *Drosophila* optic lobe to identify the genes with specific expression pattern in each subtype glia. Through bioinformatics analysis of the data, a novel ALG-specific gene (here assigned as *deathstar, des*) was identified. Immunostaining of *des* in the central nervous system (CNS)

showed its presence in specific regions of *Drosophila* brain and ventral nerve cord, previously characterized as ALG cells. Consistent with the bioinformatics analysis, *des*-related signals were overlapped with the signals of the previously-reported ALG marker. At physiological level, *RNAi*-mediated suppression of *des* gene impeded the normal development of male flies without any effects on females. Cell type-specific expression of *des* RNAi showed that *des* affects locomotion behaviour and lifespan of *D. melanogaster*, in an ALG-specific manner. Taken together, we showed that bioinformatically identified ALG-specific gene *deathstar* play critical roles in development and physiology of *Drosophila*.

KEYWORDS: Astrocyte-like glia, *CG11000*, Cell type, Male development, *Drosophila melanogaster*, Single cell RNA-seq, Specific marker, *deathstar, des*

INTRODUCTION

The brain of *D. melanogaster* is a complex organ with a diverse set of cells serving analogous functions to those of human [1]. With differential expression of the genes, each cell in the brain can determine its own fate to be a particular cell type with specific functional characteristics [2]. Previous studies have identified and reported the existence of several cell types in nervous system of *D. melanogaster* assigned as; perineural glia (PNG), subperineural glia (SPG), cortex glia (CG), neuropil ensheathing glia (EGN), tract ensheathing glia (EGT), astrocyte-like glia (ALG) and neurons (Neu) [3].

43 The function of the central nervous system (CNS) depends on a complex network of several
44 neuronal and glial cell types [4,5]. Due to the feasibility of genetic manipulation and behavioral
45 analysis, *Drosophila melanogaster* has emerged as a powerful model organism for studying the
46 development and function of the nervous system [6]. There is a functional homology between the
47 cell types in the nervous system of *D. melanogaster* and those of more advanced organisms,
48 including human. Glial cells constitute an essential part of CNS [7], and until now, several
49 distinct types of these cells were also identified in the *Drosophila* nervous system [1,3]. Each
50 cell types have a distinct profile of gene expression [8] and have their specific functions matched
51 to their physical territories or physiological states [9]. Based on the differences in gene
52 expression profile, each cell type of *Drosophila* nervous system can be distinguished by a set of
53 genes, which are known as molecular markers for each cell type [3].
54
55 In addition to the existed molecular markers for each cell type, there may be some
56 uncharacterized genes in *D. melanogaster*, which are capable of discerning a specific cell type in
57 the nervous system. Moreover, a specific cell type likely differs only in the expression of the
58 limited number of genes which confer a new function to it [10,11]. In this study, we used a
59 publicly available expression profile of 55,000 single cells of *Drosophila* optic lobe in order to
60 find novel molecular markers for specific cell types, following by experimental confirmation of
61 the predicted results.
62
63 **RESULTS**
64 **Cell type identification of the single cells of *Drosophila* optic lobe based on their specific**
65 **markers**

66 To identify the cells corresponding to distinct subtypes of glia and neurons, the expression
67 profile of the sequenced single cells by Konstantinides et al. [2] was analyzed based on their
68 previously-reported marker genes (Fig. 1A). According to the expression profile of 55000
69 sequenced single cells, the cells with the highest expression of each cell type-specific marker
70 were selected and classified. A total of forty-two cells were identified and classified into seven
71 cell types. The heatmap of gene expression for these selected cells confirmed the unique
72 expression pattern of each marker in the corresponding cell types (Fig. 1B). *CG4797* and *gem* are
73 differentially expressed in PNG, and SPG were distinguished by the three
74 markers *Mdr65*, *Moody* and *Gli*. Other glial cells were successfully distinguished by single
75 marker; *Cyp4g15*, *CG9657*, *CG34340* and *Eaat1.* Moreover, these genes could individually
76 separate CG, EGN, EGT and ALG, respectively. Neuronal cells were determined based on the
77 highest expression of *nSyb* and *elav* genes (Fig. 1B).
78

79 **Hierarchical clustering of *Drosophila* neural cell subtypes based on their similarities in**
80 **transcriptome**

81 As shown above, different types of *Drosophila* neural cells could be classified based on some
82 specific marker genes (Fig. 1). In order to know whether the classified cells in each category
83 have the same expression profile or not, correlation analysis between the selected cells was
84 carried out based on their transcriptome analysis. Results showed that most of the cells
85 expressing the same genetic marker(s) tend to be clustered together, suggesting their similar
86 transcriptome and accuracy of the identification of cell types (Fig. 2A). However, the cells with
87 the highest expression of SPG markers and some other cells could not be classified in a single
88 cluster suggesting their transcriptome dissimilarity or partial insufficiency of the available

89 genetic markers for clustering (e.g. expression heterogeneity of the SPG
90 markers: *Mdr65*, *Moody* and *Gli*).
91
92 With at least 3 out of 6 similar cells in each category, differential expression analysis was
93 performed in order to find the genes with specific expression in each cell type. While the
94 identified PNG were positive for the expression of their two known genetic markers
95 (*CG4797* and *gem*) (Fig. 1B), there were two sub-clusters of PNGs (here assigned as PNG-α and
96 PNG-β) in our transcriptome analysis which suggests the presence of a novel subtype for PNG
97 (Fig. 2A). Additional similar analysis was performed on another set of 42 cells of 55,000 cells
98 and similar clustering results were obtained, which could support the accuracy of cell type
99 characterization and clustering (Supplemental Fig.S1). The list of differentially expressed genes
100 (DEGs) for each cell type in addition to the DEGs between the two subtypes of PNG is presented
101 in Supplemental file S2.
102
103 Using the transcriptome data of the studied cell types and their clustering results, we assigned the
104 degree of differences between them as a dendrogram (Fig. 2B). Accordingly, the Venn diagram
105 was used to illustrate the number of unique and shared DEGs for each cell type. The extent of
106 unique DEGs for each cell type is as follows: 98.33% (59 of 60) for PNG, 100% (1 of 1) for
107 SPG, 90% (36 of 40) for CG, 60% (3 of 5) for EG, 78.95 (75 of 95) for ALG and 96.39 (454 of
108 471) for neurons (Fig. 2C).
109
110 **Identification of *des* as a gene with specific enrichment in astrocyte-like glia of *D.***
111 ***melanogaster***

112 After cell type identification, we asked whether specific genes can also characterize the
113 identified cell types. To identify the genes capable of distinguishing different cell types, we
114 performed differential expression analysis in order to compare the transcriptome of the cluster of
115 interest with that of all other cell types. The list of the DEGs for each cell type are presented in
116 Supplemental file S2.
117
118 Among all the clustered cells, ALG could be sufficiently discriminated by a single
119 uncharacterized gene named *CG11000* (here assigned as *deathstar, des)* [4]. Expression level
120 analysis of this gene using the RNA-seq profile of 84 single cells in *Drosophila* optic lobe [2]
121 demonstrated that among the 48 cells analyzed, 12 cells (which correspond to ALG) express *des*
122 at highest levels (Fig. 3A). In the same RNA-seq expression data (accession number:
123 GSE103771), a significant positive correlation (R^2=0.6637; *p*-value = 0.0001) was observed
124 between the expression level of the candidate gene (*des*) and that of *Eaat1*, which previously was
125 reported as an ALG-specific marker [7] (Fig. 3B). In addition, the expression pattern of *des* and
126 *Eaat1* across developmental time of *D. melanogaster*, derived from a different RNA-seq data
127 (accession number: GSE107049) showed a positive correlation between these two genes (Fig. 3C
128 and 3D), supporting the expression specificity of *des* gene in ALG of *D. melanogaster*.
129
130 To corroborate the assigned specificity of *des*, we tested whether the promoter-*GAL4* lines of this
131 gene could label ALG in CNS of *D. melanogaster*. Consistently, data showed that *des* (Red
132 signals) is mostly co-labelled with the ALG marker *Eaat1* (Green signals), in specific bilateral
133 parts of *Drosophila* optic lobe, pars intercerebrails (PI) region, and small part of subesophageal
134 ganglion (SOG) in male but not female brain (Fig. 4A). Intriguingly, *des-GAL4* identified 4-5

135 cells with large cell body towards the upper border of SOG in each hemisphere that were not
136 labeled by *Eaat1-lexA* driver (bottom panels in Fig. 4A) or previously characterized *ALG-GAL4*
137 driver [12] (Fig. 4B). We discovered that des-GAL4 further marks ALG cells in the MesoNM of
138 both male and female VNC (Fig. 4C). As shown in the brain SOG area, des-GAL4 identified 10
139 to 12 cells with large cell bodies in the ProNM/AMNp and MetaNm/ANn regions. Two of these
140 male-specific cells are uniquely designated by Eaat1-lexA, showing that male-specific des
141 expression in these distinct cell lineages (Compare MesoNm panels between male and female in
142 Fig. 4C). These cells with big cell bodies cannot be labeled using the previously published ALG-
143 GAL4 reagent [12] (Fig. 4D). All of these results indicate that *des-GAL4* identifies *Eaat1-lexA*-
144 labeled ALG cells as well as particular brain and VNC cells.
145
146 **Sex-biased developmental effect of *des* gene in *D. melanogaster***
147 We crossed GAL4 strains that are expressed in each neural cell types of *D. melanogaster* with
148 the *des-RNAi* to knockdown the expression of *des* gene in a cell type-specific manner. Our
149 results showed that most of the males expressing *des-RNAi* in all neural cell types are lethal
150 during development. However, the females with the same genotype developed normally to adult.
151 Both males and females in the control group (harboring *des-RNAi* without *GAL4* expression)
152 showed normal development (Fig. 5A). This result suggests that the *des* gene may have a
153 developmental function exclusively in male flies. However, such developmental effect was not
154 cell type-specific. As a control, the Drosophila CG15765 gene, which is less likely to express
155 with des in our analysis, was evaluated using the same methodology, and a standard male-to-
156 female ratio (~1) was obtained for all genotypes (Fig. 5B). The exact number of the progenies of
157 the corresponding crosses are summarized in the Supplemental Table S1.

158

159 **Knockdown of *des* gene affects locomotion activity of *D. melanogaster***

160 It has been previously reported that ALG cells that cover specific territories of *Drosophila* CNS
161 have significant effects on locomotion behaviours [13]. To investigate the role of *des* gene in
162 locomotion behavior in *D. melanogaster*, we knocked down the *des* gene expression through
163 expressing a *des*-specific RNAi within different cell types of *Drosophila* CNS. Then we
164 performed the climbing assay. Results showed that the flies that specifically express *des-RNAi* in
165 astrocytes exhibited significant defects in climbing ability (Fig. 6A), suggesting the crucial role
166 of this gene in this cell type. Interestingly, we found that *des* knockdown does not affect the
167 climbing activity in female flies (Fig. 6B). When we knocked down the *des* in EGN and SPG,
168 however, female flies showed severe defects in climbing activity (Fig. 6B). These data suggest
169 that the expression of *des* in ALG cells is crucial only in males, not females regarding the
170 climbing activity.

171

172 To test whether the behavioural locomotive effect of *des* gene is altered during the ageing of *D.*
173 *melanogaster*, the climbing assay was performed on the flies with different ages. Results showed
174 that the older flies (three- and four-week-old flies) expressing *des-RNAi* in all neural cell types
175 exhibited significant climbing defect (Fig. 6C). When we tested the same genotype of flies in the
176 one- and two-week stages, the climbing defects appeared in ALG-specific manner (Fig. 6C).
177 However, climbing defects were not striking for the flies with neuron-specific suppression
178 of *des*, suggesting the climbing defects related to *des* is glial-specific in old flies (Fig. 6C).
179 Unlike the male flies, both young and old females did not exhibit any meaningful pattern of

180 climbing defects (Fig. 6D). All these data suggest that the expression of *des* in male ALG cells is
181 crucial for climbing ability in the early adult stages
182

183 **Astrocyte-specific suppression of *des* gene shortens lifespan in *D. melanogaster***

184 To test the possible function of *des* gene in *D. melanogaster* lifespan, we knocked
185 down *des* expression in distinct CNS cell types (CG, PNG, ALG, EGN, EGT, SPG, Glia and
186 Neurons) and measured their life span for 40~50 days. We observed a significant reduction in
187 lifespan for the flies that had ALG-specific expression of *des* RNAi, supporting the specific
188 effect of the *des* gene in ALG on the life span of *D. melanogaster* (Fig. 7). The ALG-specific
189 effect of *des* RNAi on lifespan was observed in both male and female flies (Fig. 7A and 7B),
190 suggesting that the role of *des* on the lifespan is not sexually dimorphic. However, in the female
191 flies, such reducing effects of *des* RNAi were also observed in other cell types (EGN, EGT, PNG
192 and neurons) but at lower levels than that of ALG (Fig. 7B).

193

194 **DISCUSSION**

195 In this study, we analyzed a newly released scRNA seq dataset including typical glial cell marker
196 genes (Fig. 1) and uncovered intriguing characteristics of the *Drosophila* glial lineage (Fig. 2).
197 Among the unique marker genes revealed throughout our investigation, the *deathstar* (*des*) gene,
198 *CG11000*, might precisely designate ALG (Fig. 2). *des* expresses significantly in ALG
199 throughout early adulthood (Fig. 3). The expression of *des-GAL4* demonstrates that *des* and
200 *Eaat1* are significantly coexpressed in the adult head and VNC (Fig, 4). *des* gene knockdown

201 using subtype-specific glia-*GAL4s* reveals glial roles of *des* throughout development (Fig. 5),
202 adult locomotion (Fig. 6), and lifetime (Fig. 7).
203
204 Recent advances of single-nuclear RNA-sequencing (snRNA-seq) technologies enable fly
205 community to establish a cell atlas for the entire adult *Drosophila* [14]. Using the publicly
206 accessible Fly Cell Atlas annotation dataset in SCope website, we examined the expression
207 patterns of *deathstar* (*des*) in several tissues with distinct annotations. In the entire tissues of both
208 male and female flies, the expression of *des* strongly overlapped with glial cells (yellow dots in
209 Fig. S2A-B). *des* expression is also detectable in annotated neurons (magenta dots in Fig. S2C-
210 D). When consolidated, tiny clusters of glial cells could be distinguished from neurons (black-
211 dotted circles in Fig. S2E-F).
212
213 To determine the ALG expression of *des*, we employed the previously identified ALG markers
214 *astrocytic leucine-rich repeat molecule* (*alrm*) and *Eaat1*. The SCope platform does not yet
215 support well-defined ALG annotations. Intriguingly, the glial cell clusters observed in Fig. S1E-
216 F were also recognized by *alrm* (Fig. S3A-B) and *Eaat1* (Fig. S3C-D) in all tissues. We believe
217 that these tiny clusters are ALG cells in adult flies. This ALG cluster starts to be appeared from
218 the 3 days old adult stage (Fig. S2G-J). The head exhibited more ALG cells than the entire body
219 (Figure S3E-H), and the annotated glial cells in SCope demonstrate co-expression of *des* with
220 *alrm* and *Eaat1* in a unique ALG cluster (Fig. S3I-J).
221
222 To investigate if this unique cluster of cell types is ALG, we examined every subtype of glial cell
223 identified in SCope. The ALG clusters in the head (gray-dotted region in Fig. S4) did not overlap

224 with neuron (Fig. S4A-B), adult brain cell body glial cell (Fig. S4C-D), adult brain perineurial
225 glial cell (Fig. S4E-F), adult lamina epithelial/marginal glial cell (Fig. S4G-H), adult optic
226 chiasma glial cell (Fig. S4O-P). The ALG cluster in the body (gray-dotted region in Fig. S5) did
227 not overlap with neuron (Fig. S5A-B), CNS surface associated glial cell (Fig. S5C-D), cell body
228 glial cell (Fig. S5E-F), subperineurial glial cell (Fig. S5G-H), and perineurial glial sheath (Fig.
229 S5I-J). However, we found that *des* expression pattern in the body overlaps with adult reticular
230 neuropil associated glial cell (Fig. S5K-L). These data suggest that our bioinformatics analysis of
231 ALG-associated *des* expression is also confirmed by FCA dataset. We believe the *des*-specific
232 ALG cluster in the body represents the *des-GAL4*-labeled large cell body cells in the brain and
233 VNC (Fig. 4).
234
235 There are pieces of evidence for ALG-enriched gene that have different patterns of expression
236 during early and late stages of *D. melanogaster* development. ALG-enriched genes in larval
237 stages are mainly involved in metabolism, energy production, and protein synthesis, consistent
238 with the known role of astrocytes in metabolic support of neurons. In comparison with the larval
239 astrocytes, ALG cells in adult *D. melanogaster* acquire a new function for regulation of
240 behaviors, additional to their functions in earlier stages [15]. Therefore, it is expected that the
241 suppression of the *des* gene in larval stages is lethal in males. However, this suppression at
242 adulthood stages mediates climbing defects in males (Fig. 5 and 6). In accordance of this idea,
243 the *des* protein has a 'Pleckstrin homology domain' (PH domain). PH domain can bind
244 phosphatidylinositol within biological membranes and proteins, such as the beta/gamma subunits
245 of heterotrimeric G proteins and protein kinase C, and play a role in recruiting proteins to

246 different membranes, thereby targeting them to appropriate cellular compartments or allowing
247 them to interact with other components of signal transduction pathways [16].
248
249 Analysis of lifespan in the flies expressing *des* RNAi in different cell types showed the greatest
250 effects when *des* is suppressed specifically in ALG cells which was observed in both sexes,
251 providing another supportive evidence for specificity of the gene to ALG cell type (Fig. 7). It is
252 known that *Drosophila* astrocytes (ALG) are significant contributors to modulate
253 neurotransmitter homeostasis within synapses [17] and also regulators of circadian rhythm [18].
254 Therefore, it is likely that abolishing the functions of ALG or ALG-specific genes could interfere
255 with normal locomotion properties and lifespan of *D. melanogaster*, which are the direct
256 outcome of dysregulations in neurotransmission and circadian rhythm, respectively. Moreover, it
257 was recently reported that mitochondrial dysfunctions in ALG cells contribute to
258 neurodegeneration [17,19], which could give rise to shortened lifespan of *D. melanogaster* [20].
259
260 Taken together, *des* (previously known as *CG11000*) was reported as a protein-coding gene in
261 fruit fly with 332 amino acids. Its functional role was not known yet in *Drosophila*, and it has no
262 homologue gene in human. However, it is predicted to be involved in regulation of cell
263 differentiation process (Flybase). In this study, we firstly annotated *des* as an ALG-specific gene
264 which could mediate the developmental process of the male flies additional to its functions in
265 locomotion and lifespan properties of *D. melanogaster*. Further investigations will shed insight
266 on how this membrane protein with a PH domain may specify the identity of ALG from neurons
267 and influence *Drosophila* physiology.
268

269 **MATERIALS AND METHODS**

270 **Dataset**

271 A single-cell RNA-sequencing (RNA-seq) data of a recently published paper [2] was selected
272 from the data repository NCBI Gene Expression Omnibus (GEO) (accession number:
273 GSE103771). It contained the expression profile of 17272 *Drosophila* genes in a population of
274 55000 single cells from the optic lobe of *Drosophila* brain. Also, the data of expression profile
275 for the whole brain of *D. melanogaster* across four different developmental stages (days 5, 10, 20
276 and 40 after eclosion) were downloaded from NCBI GEO (accession number: GSE107049).

277

278 **Bioinformatics analyses**

279 For expression analysis of the genes in single cells of *D. melanogaster* brain, the expression
280 matrix belonging to the study of Konstantinides et al. [2] was downloaded for downstream
281 analyses. We analyzed the expression matrix of the single cell RNA-seq data of *Drosophila* optic
282 lobe (accession number: GSE103771) based on the expression level of known markers,
283 previously reported for each cell type. Based on the expression pattern of the specific markers,
284 the type of the cells in the matrix was characterized. For each cell type, six single cells were
285 selected according to the expression level of the markers. Forty-two cells comprising seven cell
286 types of *Drosophila* nervous system (assigned as perineural glia (PNG), subperineural glia
287 (SPG), cortex glia (CG), neuropil ensheathing glia (EGN), tract ensheathing glia (EGT),
288 astrocyte-like glia (ALG) and neurons (Neu)) were selected for downstream analyses. For
289 confirmation of this cell type classification, hierarchical clustering was performed for the
290 selected forty-two cells based on their similarities in transcriptome and presented as a heatmap
291 with color codes for the Pearson correlation coefficient. The clusters with at least three cells (of

292 all six cells) were validated as unique cell type. For further confirmation, this analysis was
293 performed similarly on another set of forty-two cells from the 55,000 single cells. To identify the
294 genes enriched in a specific cell type, we first identified differentially expressed genes (DEGs)
295 between the examined cell types and all other cells by the R package limma [21]. Then, after
296 applying adjusted *P*-values (Benjamini–Hochberg correction) of < 0.05 and $\log_2 FC \geq 1.5$, the
297 specificity of the candidate genes with highest degree of enrichment was determined by analysis
298 of their expression across all the examined single cells (unpaired t-test; *P*-value < 0.05). Venn
299 diagram was obtained from the web-based tool on
300 http://bioinformatics.psb.ugent.be/webtools/Venn/.
301

302 **Fly stocks and crosses**

303 All the *Drosophila melanogaster* lines in this study were prepared from Bloomington Drosophila
304 Stock Center (BDSC). After receiving the stocks, they were cultured in standard conditions
305 (standard cornmeal-agar yeast fly food at 25° C on a 12-h light:12-h dark condition) as
306 previously described [22]. CO_2 was used as an anesthetic. For functional analysis of the genes,
307 the *GAL4/UAS-RNAi* system was used to deplete their functions in a cell-type specific manner.
308 The fly stocks together with their crosses for functional analyses of *des* gene are summarized in
309 table 1. After crossing the virgin females of *UAS-des*-RNAi line with males of different GAL4
310 driver lines (*X-GAL4*), ensuring expression of RNAi in cell type-specific manner, the transgenic
311 progenies (*X-GAL4 > UAS-RNAi*) were collected based on their genotypes and assessed for their
312 behaviors (Table 1). The specific *GAL4* driver gene for each cell type was as below: *CG4797*
313 gene for PNG, *Mdr65* gene for SPG, *Cyp4g15* gene for CG, *CG9657* gene for EGN, *CG34340*
314 gene for EGT, *Eaat1* gene for ALG, *repo* gene for all glial cells (glia) and *nSyb* gene for

315 neurons. For control of the experiment flies without expression of RNAi were used. These flies
316 had *RNAi* in their genome without expression of *GAL4*. Therefore, no functional *RNAi* was
317 produced in the control flies. All of our experiments were performed in Canton-S/wild type
318 background to rule out all the genetic background effects.
319
320 For the crosses of fluorescent labeling experiments, the two binary systems of *GAL4/UAS-*
321 *mCD8GFP* and *LexA/LexAoP-mCD8RFP* were used simultaneously in an individual male and
322 female flies. The ALG cells of *Drosophila* CNS were labelled by the expression of a membrane-
323 bound GFP (*mCD8GFP*) under the control of *Eaat1* gene promoter, fused to the sequence of
324 *LexA* (*Eaat1*-LexA). For tracing the expression pattern of *des* gene in *Drosophila* CNS, a
325 transgenic fly line carrying *des-GAL4* construct (BDSC#: 23418) was used. Expression of RFP
326 under the control of *des* gene promoter depicts the expression distribution of *des* gene across
327 CNS. The crossing scheme for this experiment is summarized in table 2.
328
329 **Immunostaining and imaging**
330 As described before [21], brains dissected from adults 5 days after eclosion were fixed in 4%
331 formaldehyde for 30 min at room temperature, washed with 1% PBT three times (30 min each)
332 and blocked in 5% normal donkey serum for 30 min. The brains were then incubated with
333 primary anti-bodies in 1% PBT at 4° C overnight followed with fluorophore-conjugated
334 secondary antibodies for 1 hour at room temperature. Brains were mounted with antifade
335 mounting solution (Invitrogen, catalog #S2828) on slides for imaging.
336

337 Primary antibodies used here are chicken anti-GFP (Aves Labs, 1:1000), rabbit anti-DsRed
338 express (Clontech, 1:250) and mouse anti-Bruchpilot (nc82) (DSHB, 1:50). Fluorophore-
339 conjugated secondary antibodies used here are Alexa Fluor 488-conjugated goat anti-chicken
340 (Invitrogen, 1:100). Alexa Fluor 488-conjugated donkey anti-rabbit (Invitrogen, 1:100), RRX-
341 conjugated donkey anti-rabbit (Jackson Laboratory, 1:100), and Dylight 405-conjugated donkey
342 anti-mouse (Jackson Laboratory, 1:100).
343
344 Images were collected using a Zeiss LSM 7 MP microscope scanning confocal microscope.
345 Projection of the confocal stacks, adjusting the brightness and contrast of the images were
346 performed by NIH ImageJ [26], then presented by Adobe Illustrator CC 2019 for windows.
347
348 **Developmental lethality assays**
349 To assess the possible function of *des* gene in the development of *D. melanogaster* from pupae to
350 adulthood stage, the newly eclosed *D. melanogaster* adults of the crosses in Supplemental Table
351 1, were collected and counted based on their genotypes. After counting, data were presented as
352 the percentage of male and female flies with *des* RNAi to the total number of eclosed flies.
353
354 **Lifespan assay**
355 Lifespan was measured at room temperature according to standard protocols. In brief, newly
356 ecloded flies (0 to 3 days) were collected (50 per genotype) and then placed in vials (25 flies per
357 vial) and transferred to fresh vials every three days. Survival was recorded for each genotype
358 (two vials). We scored flies stacked in the food as death events in all the vials analyzed. We
359 created survival curves with Prism version 6 (GraphPad Software, San Diego, CA, USA) using

360 the method of Kaplan and Meier. For statistical significance of the experiment, one-way
361 ANOVA method was used and the death rate of each genotype was compared to the Canton-S
362 (CS) flies as the control. *P-value < 0.05, ** P-value < 0.01.
363
364 **Climbing assay**
365 For the climbing assay, flies were separated into groups of 25 adults per each vial and kept in 29°
366 C. At the time of experiment, the groups of 25 flies were placed in an empty climbing vial and
367 then tapped down to the bottom. They were allowed to climb from the bottom to top of the vial
368 (8 cm) for 20 seconds. In order to evaluate the climbing pattern of each genotype, the climbing
369 height achieved by each genotype was calculated in every 5 seconds after the tapping and
370 initiating negative geotaxis. The results of climbing assay were obtained by video recording of
371 climbing flies then processed by ImageJ software. Data was presented as graphs using Prism
372 version 6 (GraphPad Software, San Diego, CA, USA). Flies with wild-type/*UAS-RNAi* genotype
373 were used as control group.
374
375 **Statistical analysis**
376 Statistical analysis and graphic representations were performed using Prism 6.00 for Windows
377 (GraphPad Software, San Diego, CA, USA). Unpaired t test or one-way ANOVA (using the
378 Bonferroni's multiple comparison) were applied depending on the measurements analyzed in the
379 corresponding experiment. In all cases averages with SEM are plotted. P-values were calculated
380 by two-tailed unpaired Student's t-test unless otherwise specified, using GraphPad Prism 6
381 software. All data are presented as the mean ± SEM. $*P < 0.05$; $**P < 0.01$; and $***P < 0.001$.
382

383 **Single-nucleus RNA-sequencing Analyses - Data and Code Availability**

384 snRNAseq dataset analyzed in this paper is published in [14] and available at the Nextflow
385 pipelines (VSN, https:// github.com/vib-singlecell-nf), the availability of raw and processed
386 datasets for users to explore, and the development of a crowd-annotation platform with voting,
387 comments, and references through SCope (https://flycellatlas.org/ scope), linked to an online
388 analysis platform in ASAP (https://asap.epfl.ch/fca).

389

390 **Gene expression pattern analyses in different tissues**

391 For the gene expression pattern of the 10 genes involved in SMD in each cell type of leg and
392 other tissues, we used the single-cell RNA-seq data from https://flycellatlas.org [14], and the 10x
393 Genomics stringent loom files were downloaded. The cell types are split by FCA.

394 The digital expression matrices were analyzed with the Seurat 4.1.0 R package [23]. The dot
395 plots of the 10 genes involved in SMD in each cell type of different tissues were then made using
396 the 'DotPlot' function with broad annotation (broad cell types) and the annotation (detailed cell
397 types), respectively.

398

399 **LIST OF ABBREVIATIONS**

400 **ALG**: Astrocyte-like glia; **BBB**: Blood-brain barrier; **CG**: Cortex glia; **CNS**: Central nervous
401 system; **CS**: Canton S; **DEG**: Differentially-expressed gene; **dsRNA**: double strand RNA; **EGN**:
402 Neuropil ensheathing glia; **EGT**: Tract ensheathing glia; **GEO**: Gene expression Omnibus**;**

403 **NEU**: Neurons; **PNG**: Perineural glia; **RNAi**: RNA interference; **SPG**: Subperineural glia; **GFP**:
404 Green fluorescent protein; **RFP**: Green fluorescent protein.
405

406 **DECLARATIONS**

407 **Ethics approval and consent to participate:** Not applicable.

408 **Consent for publication:** Not applicable.

409 **Availability of data and materials:** Not applicable.

410 **Competing interests:**

411 The authors declare that they have no competing interests.

412 **Funding:** This research was supported a University of Ottawa Startup grant to WJK, a
413 University of Ottawa Brain and Mind Research Institute/Center for Neural Dynamics Open call
414 project grant to WJK, a University of Ottawa Interdisciplinary Research Group Funding
415 Opportunity (IRGFO stream 1 and 2) Grant to WJK, a Natural Sciences and Engineering
416 Research Council of Canada (NSERC) Discovery grant (reference: 211406) to WJK, a Mitacs
417 Globalink Research Internship Program grant to WJK, and Startup funds from HIT Center for
418 Life Science to WJK. This research was also supported by the Brain Pool Program of the
419 National Research Foundation in Korea to WJK, Burroughs Wellcome Fund Collaborative
420 Research Travel Grants (reference: 1017486) to WJK and a NVIDIA Academic Hardware Grant
421 Program to WJK.

422

423 **AUTHOR CONTRIBUTIONS:**

Concept and design of experiments: WJK, HN and KW; performing the experiments: HN, KW, WJK and AS; acquisition of data: HN, KW, WJK and AS; analysis and interpretation of data: HN, KW and WJK; revision experiments and analysis: HM; drafting or revising the article: HN and WJK.

ACKNOWLEDGMENTS:

Stocks obtained from the Bloomington Drosophila Stock Center (NIH P40OD018537) were used in this study. We also thank Khoi-Nguyen Ha Nguyen for his contribution to experiments performed in this manuscript.

FIGURE LEGENDS

Figure 1. Identification of *Drosophila* neural cell types through analysis of their specific marker genes. (A) Specific marker genes, previously reported as markers for each cell type of *Drosophila* glial cells. (B) Heatmap shows the expression pattern of the markers across 42 selected cells from 55000 single sequenced cells, in which, six different cells were identified as a unique cell type (denoted by different colors). Cells' numbers correspond to the numbering method of Konstantinides et al. Red and black colors indicate the marker-positive and marker-negative cells, respectively. Color intensities in the heatmap denote the level of gene expression based on RPKM per single cell.

444 **Figure 2. Hierarchical clustering of different neural cell types of *D. melanogaster* based on**
445 **their transcriptome. (**A) Hierarchical cluster analysis of gene expression for 42 selected cells
446 from *Drosophila* optic lobe based on the expression level of 17,272 genes for each single cell.
447 Except SPG, all the studied cell types were clustered together suggesting their similarities in
448 expression profile. PNG cells were strongly clustered in two different clusters, suggesting
449 presence of two distinct PNG subtypes in *Drosophila* (PNG-α and PNG-β). (B) Dendrogram
450 shows the similarity degree of the clustered cells based on whole transcriptome. (C) Number of
451 unique and shared DEGs for each cell type of *D. melanogaster* nervous system. Total number of
452 DEGs for each cell type are presented in parenthesis. PNG= perineural glia, SPG= subperineural
453 glia, CG= cortex glia, ALG= astrocyte-like glia, EG= ensheathing glia, and NEU= neurons.

454

455 **Figure 3. Expression specificity of *des* gene in ALG cells of *D. melanogaster*. (**A) While the
456 ALG cells exhibited high level of *des* mRNA (Blue points), other glia cells as well as neurons
457 showed low or no expression of this gene (gray points). (B) Positive correlation between
458 expression level of known ALG marker (*Eaat1* gene) and that of *des* gene. Blue and gray points
459 respectively denote expression of the genes in ALG and non-ALG single cells. (C) Similar
460 expression pattern of *des* (dark blue) and *Eaat1* (bright blue) genes during development of male
461 *D. melanogaster*. (D) Similar expression pattern of *des* (dark blue) and *Eaat1* (bright blue) genes
462 during development of female *D. melanogaster*. Developmental times are presented as the days
463 after eclosion of the flies. SPG= subperineural glia, PNG= perineural glia, CG= cortex glia,
464 ALG= astrocyte-like glia, EGN= neuropil ensheathing glia, EGT= tract ensheathing glia, and
465 NEU= neurons.

466

467 **Figure 4. *des* gene is sex-specifically expressed in *Drosophila* ALG cells.** Immunostaining
468 result of (A) brain and (C) VNC in male and female flies. In both images, the ALG cells were
469 stained with anti-GFP (green), and the red signals (anti-RFP) reflect *UAS-mCD8RFP* driven by a
470 *GAL4*, tagged by the promoter region of *des* gene (*des-GAL4*). Anti-nc82 was used to label
471 neuropil (Blue). Co-labeling of astrocytic cells using *Eaat1-lexA/lexAop-mCD8GFP* (green)
472 together with *des-GAL4/UAS-mCD8RFP* (Red) showed ALG-specific expression of *des* gene
473 among other types of *Drosophila* glia cells. Scale bars represent 100 µm in top panels and 50 µm
474 in others. Dotted boxes represent the magnified area in the next panels. Dotted entangles indicate
475 the regions of *des*-positive and *Eaat1*-positive cells found. Red arrows indicate des-positive but
476 Eaat1-negative large cell body cells and Empty red-line arrows indicate those cells are empty in
477 Eaat1-lexA/lexAop-mCD8GFP panels. (B and D) Female (B) brain and (D) VNC of flies
478 expressing ALG-GAL4/UAS-mCD8GFP. Source image lsm files (~500MB) were downloaded
479 from FlyLight platform constructed by Janelia Farm Research Center (JFRC) then reconstructed
480 using ImageJ https://www.janelia.org/project-team/flylight. PI: pars intercerebrails; OL: optic
481 lobe; SOG; subesophageal ganglion; VNC; ventral nerve cord; ProNm: Prothoracic neuromere;
482 AMNp: Accessory Mesothoracic neuropil; MesoNm: Mesothoracic neuromere; MetaNm:
483 Metathoracic neuromere; ANm: bdominal neuromere [24].

484

485 **Figure 5. Male-specific developmental effect of *des* gene in *D. melanogaster*. (**A) While the
486 females with *des-RNAi* showed normal development, male flies with the same genotypes could
487 not be matured to adults and showed overall less frequencies in comparison with the expected
488 ratio of each genotype. (B) Using another RNAi as control (*CG15765* RNAi), equal number of
489 males and females were observed which were consistent with the expected ratio of each

490 genotype. $*P < 0.05$; $**P < 0.01$; $***P < 0.001$ and $****P < 0.0001$, n.s.= non-significant ($P \geq$

491 0.05).

492

493 **Figure 6. Effects of *des* gene suppression on locomotion behavior of *D. melanogaster*. (**A)

494 ALG-specific reduction of climbing activity in male flies under suppression of *des* gene. (B)

495 Slight EGN- and SPG-specific reduction of climbing behavior in female *D. melanogaster* under

496 suppression of *des* gene. (C) Climbing behaviors of male *D. melanogaster* expressing *des* RNAi

497 during different times of development (weeks 1-4 post-eclosion) showing ALG-specific effect of

498 the gene. (D) Climbing behaviors of female *D. melanogaster* expressing *des* RNAi during

499 different times of development (weeks 1-4 post-eclosion) showed no significant effect in ageing

500 flies.

501

502 **Figure 7. Lifespan effect of *des* gene suppression in *D. melanogaster*.** Suppression of *des* gene

503 shortened lifespan of male and female flies in an ALG-specific manner. Only the males with

504 ALG-specific suppression of *des* showed significant reduction in survival. In females, the

505 greatest level of lifespan reduction was observed for the flies with ALG-specific suppression of

506 *des*. However, females carrying *des* RNAi in their EGN, EGT, PNG and neurons showed such an

507 effect with lower extent. CS refers wild-type/*des-RNAi* control flies.

508

509 **SUPPLEMENTARY FIGURE LEGENDS**

510 **Figure S1. Hierarchical clustering of single cells selected based on specific markers for**
511 **neural cell types of *D. melanogaster*.** Among all cell types, the ALG and neurons had the best
512 clustering pattern.

513

514 **Figure S2.** Whole tissue Fly SCope dataset. (A-F) Annotations and gene names are color-coded
515 using red, green, and blue words. When cells overlap, the color of the dots is either yellow, cyan,
516 or magenta. Colored arrows indicate cells that have been double- or triple-labeled by annotations
517 and genes. (G-J) Whole tissue Fly SCope dataset in day1, 2, 3, and 5 with the expression of *des,*
518 *alrm,* and *Eaat1*.

519

520 **Figure S3.** Fly SCope dataset. (A-J) Tissues, sexes, annotations and gene names are color-coded
521 using red, green, and blue words. When cells overlap, the color of the dots is either yellow, cyan,
522 or magenta. Dotted entangles indicate probabl cell populations of *des*-positive ALG cells.

523

524 **Figure S4.** Head region of Fly SCope dataset. (A-P) Tissues, sexes, annotations and gene names
525 are color-coded using red, green, and blue words. When cells overlap, the color of the dots is
526 either yellow, cyan, or magenta. Dotted entangles indicate probabl cell populations of *des*-
527 positive ALG cells.

528 **Figure S5.** Body region of Fly SCope dataset. (A-L) Tissues, sexes, annotations and gene names
529 are color-coded using red, green, and blue words. When cells overlap, the color of the dots is

530 either yellow, cyan, or magenta. Dotted entangles indicate probabl cell populations of *des*-
531 positive ALG cells.

532

533 **Table 1. Summary of crosses and experimental genotypes for behavioral analyses.** In order
534 to generate the transgenic flies with expression of *des*-RNAi in cell type-specific manner, the
535 male flies of different *GAL4* driver lines were crossed with the females harboring *des*-dsRNAi in
536 their genome (BDSC#: 51918). All the females (♀) for these crosses were virgin. Among the
537 progenies of these crosses, the flies with proper genotypes were selected based on the absence of
538 balancer chromosomes (CyO, TM3 and TM6B).

539

540 **Table 2. Crossing scheme for imaging experiments of CNS in *Drosophila*.** The line A
541 contains RFP and GFP reporter genes under regulation of UAS and LexAop sequences,
542 respectively. Line B expresses lexA protein in an ALG-specific manner. By crossing the lines A
543 and B (Parents), the fly line C (F_1 generation) was produced and then crossed with *des-GAL4*
544 line (D) to produce F_2 generation. Among the flies of F_2, the males and females that lack
545 balancer chromosomes but contain the components of the binary systems *UAS/GAL4* and
546 *LexA/LexAop* were selected for central nervous system (CNS) dissection. The females (♀) of all
547 crosses were virgin.

548

549 **SUPPLEMENTAL DATA CAPTIONS**

550 **Supplemental file 1. List of differentially expressed genes for each cell type of *Drosophila***

551 **central nervous system.** The genes with $\log_2$fold change (Log_2FC) ≥ 1.5 and *P*-value < 0.05

552 were considered as differentially expressed genes (Denoted as highlighted cells).

553

554 **Supplemental Table 1. Number of newly-eclosed flies under suppression of *des* gene in**

555 **neural cell types of *D. melanogaster*.** The number of male progenies was less than the females

556 when the *des* expression was suppressed in neural cell types of *D. melanogaster* (RNAi carriers).

557 As control of the experiment, a fly line which had no expression of *des* RNAi (referred as

558 balancer carrier) was used. Equal number of males and females was observed for this control

559 (CS) group.

560

561 **REFERENCES**

562

563 1. Freeman MR. Drosophila central nervous system glia. Cold Spring Harbor perspectives in
564 biology. 2015;7: a020552.

565 2. Konstantinides N, Kapuralin K, Fadil C, Barboza L, Satija R, Desplan C. Phenotypic
566 convergence: distinct transcription factors regulate common terminal features. Cell. 2018;174:
567 622-635. e13.

568 3. Kremer MC, Jung C, Batelli S, Rubin GM, Gaul U. The glia of the adult D rosophila nervous
569 system. Glia. 2017;65: 606–638.

570 4. Zeng Z, Miao N, Sun T. Revealing cellular and molecular complexity of the central nervous
571 system using single cell sequencing. Stem cell research & therapy. 2018;9: 234.

572 5. Brody T, Odenwald WF. Cellular diversity in the developing nervous system: a temporal view
573 from Drosophila. Development. 2002;129: 3763–3770.

574 6. Olesnicky E, Wright E. Drosophila as a model for assessing the function of RNA-binding
575 proteins during neurogenesis and neurological disease. Journal of developmental biology.
576 2018;6: 21.

577 7. Yildirim K, Petri J, Kottmeier R, Klämbt C. Drosophila glia: Few cell types and many
578 conserved functions. Glia. 2019;67: 5–26. doi:10.1002/glia.23459

579 8. Shih M-FM, Davis FP, Henry GL, Dubnau J. Nuclear transcriptomes of the seven neuronal
580 cell types that constitute the Drosophila mushroom bodies. G3: Genes, Genomes, Genetics.
581 2019;9: 81–94.

582 9. Croset V, Treiber CD, Waddell S. Cellular diversity in the Drosophila midbrain revealed by
583 single-cell transcriptomics. Elife. 2018;7: e34550.

584 10. Henry GL, Davis FP, Picard S, Eddy SR. Cell type–specific genomics of Drosophila neurons.
585 Nucleic acids research. 2012;40: 9691–9704.

586 11. Hilu-Dadia R, Hakim-Mishnaevski K, Levy-Adam F, Kurant E. Draper-mediated JNK
587 signaling is required for glial phagocytosis of apoptotic neurons during Drosophila
588 metamorphosis. Glia. 2018;66: 1520–1532.

589 12. Kremer MC, Jung C, Batelli S, Rubin GM, Gaul U. The glia of the adult Drosophila nervous
590 system. Glia. 2017;65: 606–638. doi:10.1002/glia.23115

591 13. Peco E, Davla S, Camp D, Stacey SM, Landgraf M, Meyel DJ van. Drosophila astrocytes
592 cover specific territories of the CNS neuropil and are instructed to differentiate by Prospero, a
593 key effector of Notch. Development. 2016;143: 1170–1181.

594 14. Li H, Janssens J, Waegeneer MD, Kolluru SS, Davie K, Gardeux V, et al. Fly Cell Atlas: A
595 single-nucleus transcriptomic atlas of the adult fruit fly. Science. 2022;375: eabk2432.
596 doi:10.1126/science.abk2432

597 15. Liu L, Zhang K, Sandoval H, Yamamoto S, Jaiswal M, Sanz E, et al. Glial lipid droplets and
598 ROS induced by mitochondrial defects promote neurodegeneration. Cell. 2015;160: 177–190.

599 16. Wang DS, Shaw R, Hattori M, Arai H, Inoue K, Shaw G. Binding of Pleckstrin Homology
600 Domains to WD40/β-Transducin Repeat Containing Segments of the Protein Product of the Lis-
601 1 Gene. Biochem Bioph Res Co. 1995;209: 622–629. doi:10.1006/bbrc.1995.1545

602 17. Kounatidis I, Chtarbanova S. Role of glial immunity in lifespan determination: a Drosophila
603 perspective. Frontiers in immunology. 2018;9: 1362.

604 18. Ritchie ME, Phipson B, Wu D, Hu Y, Law CW, Shi W, et al. limma powers differential
605 expression analyses for RNA-sequencing and microarray studies. Nucleic acids research.
606 2015;43: e47–e47.

607 19. Guo A, Li L, Xia S, Feng C, Wolf R, Heisenberg M. Conditioned visual flight orientation in
608 Drosophila: dependence on age, practice, and diet. Learning & Memory. 1996;3: 49–59.

609 20. Brand AH, Perrimon N. Targeted gene expression as a means of altering cell fates and
610 generating dominant phenotypes. development. 1993;118: 401–415.

611 21. Kim WJ, Jan LY, Jan YN. A PDF/NPF Neuropeptide Signaling Circuitry of Male Drosophila
612 melanogaster Controls Rival-Induced Prolonged Mating. Neuron. 2013;80: 1190–1205.
613 doi:10.1016/j.neuron.2013.09.034

614 22. Schneider CA, Rasband WS, Eliceiri KW. NIH Image to ImageJ: 25 years of image analysis.
615 Nature methods. 2012;9: 671.

616 23. Satija R, Farrell JA, Gennert D, Schier AF, Regev A. Spatial reconstruction of single-cell
617 gene expression data. Nat Biotechnol. 2015;33: 495–502. doi:10.1038/nbt.3192

618 24. Court R, Namiki S, Armstrong JD, Börner J, Card G, Costa M, et al. A Systematic
619 Nomenclature for the Drosophila Ventral Nerve Cord. Neuron. 2020;107: 1071-1079.e2.
620 doi:10.1016/j.neuron.2020.08.005

621

A

Cell type	Marker gene
PNG	CG4797
	gem
SPG	Mdr65
	moody
	Gli
CG	Cyp4g15
EGN	CG9657
EGT	CG34340
ALG	Eaat1
NEU	nSyb
	elav

- PNG: Perineurial glia
- CG: Cortex glia
- SPG: Subperineurial glia
- EGN: Neuropile ensheathing glia
- EGT: Tract ensheathing glia
- ALG: Astrocyte-like glia
- NEU: Neurons

B

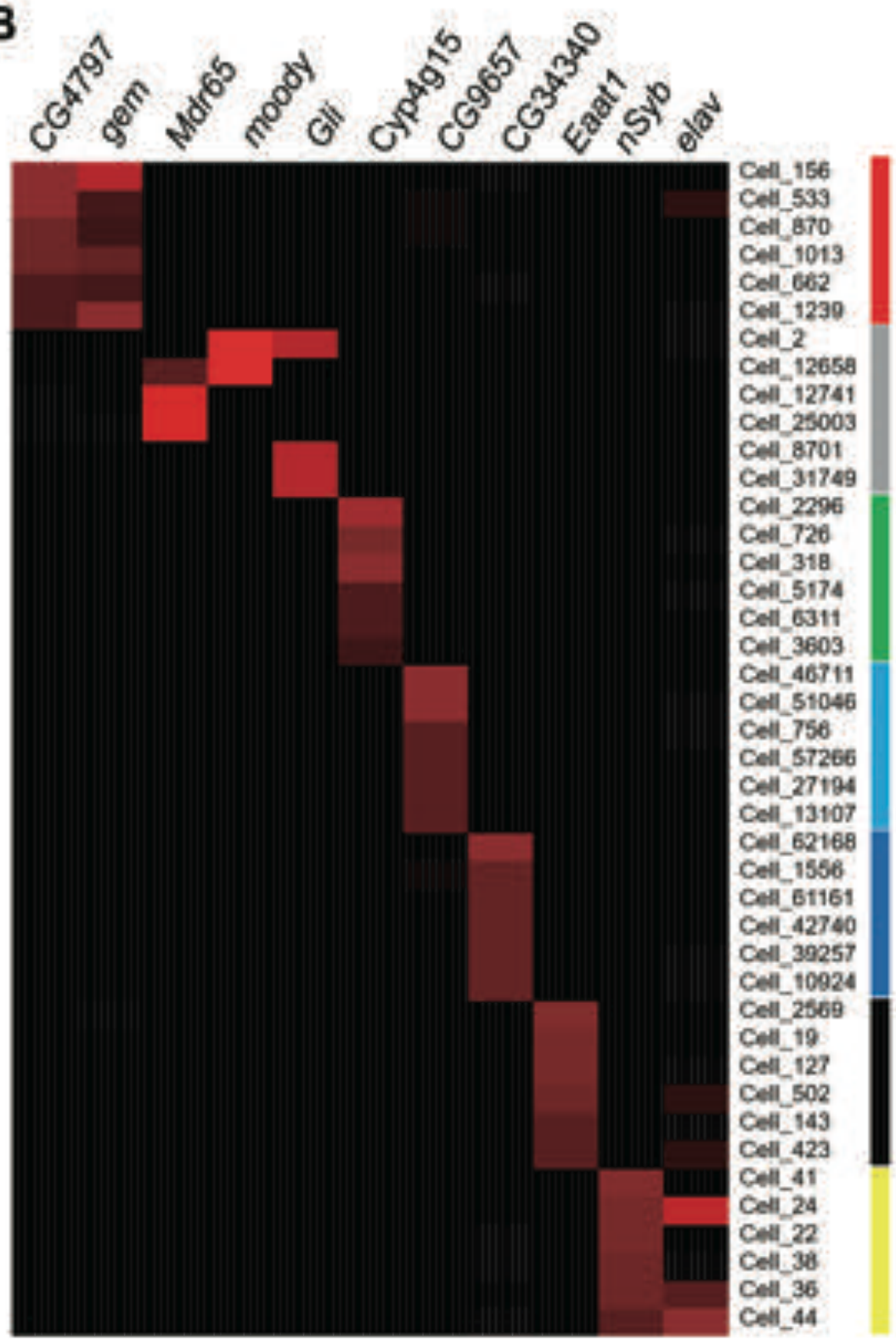

Hadi., Fig.1

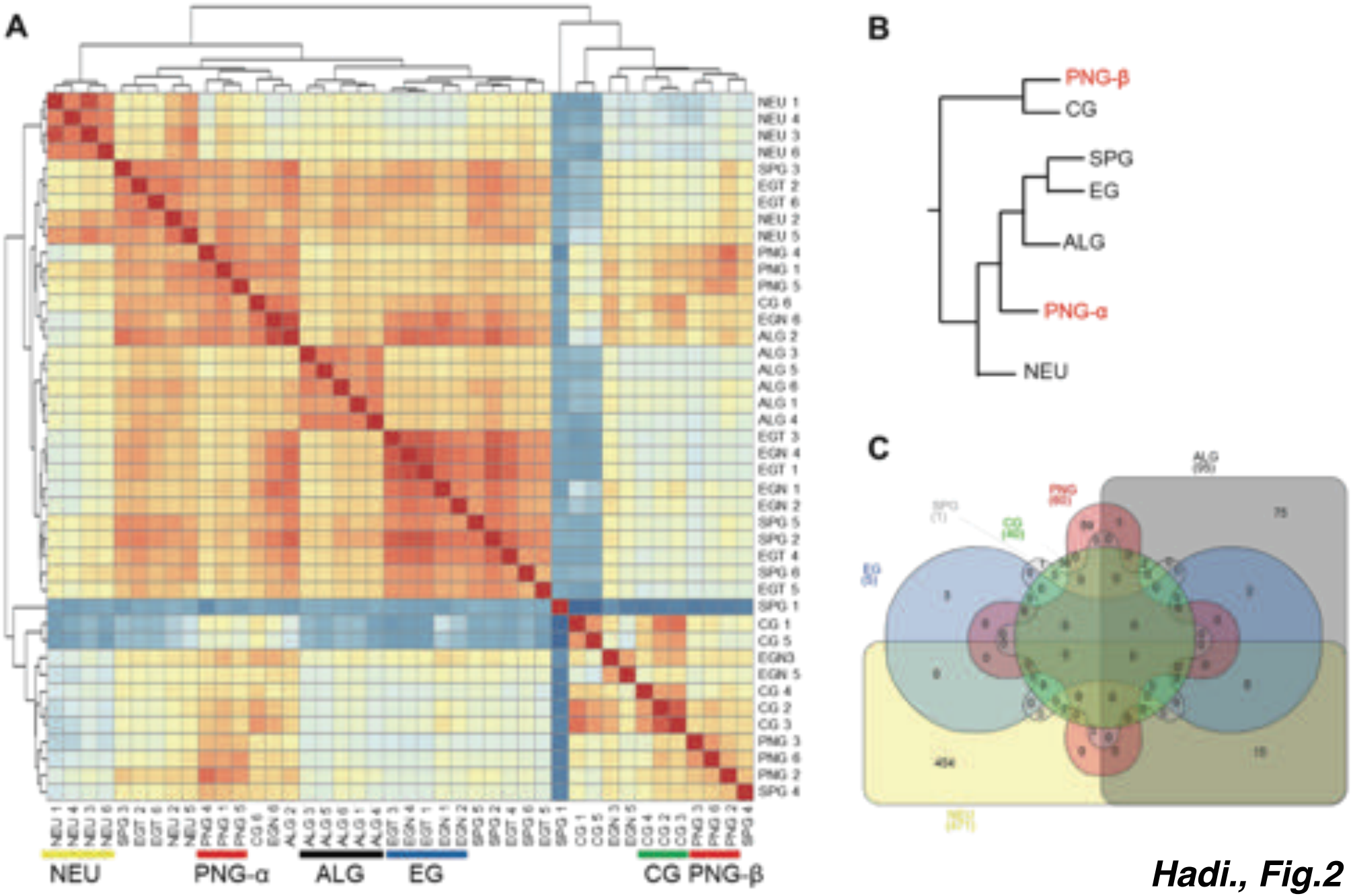

Hadi., Fig.2

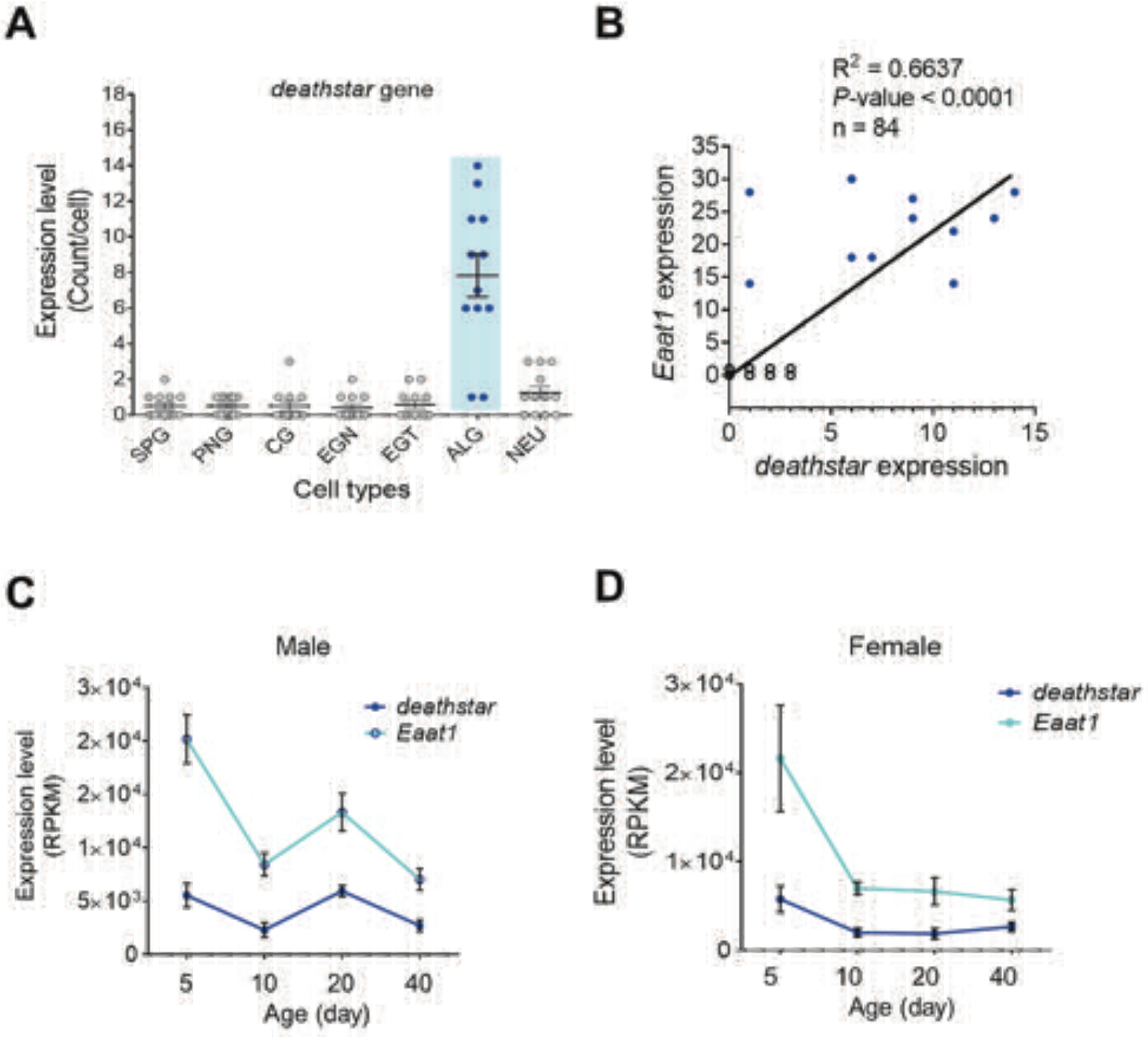
A
deathstar gene
Expression level (Count/cell)
18
16
14
12
10
8
6
4
2
0
SPG
PNG
CG
EGN
EGT
ALG
NEU
Cell types
B
R2 = 0.6637
P-value < 0.0001
n = 84
Eaat1 expression
35
30
25
20
15
10
5
0
0
5
10
15
deathstar expression
C
Male
Expression level (RPKM)
3×10⁴
2×10⁴
2×10⁴
1×10⁴
5×10³
0
deathstar
Eaat1
5
10
20
40
Age (day)
D
Female
Expression level (RPKM)
3×10⁴
2×10⁴
1×10⁴
0
deathstar
Eaat1
5
10
20
40
Age (day)

Hadi., Fig.3

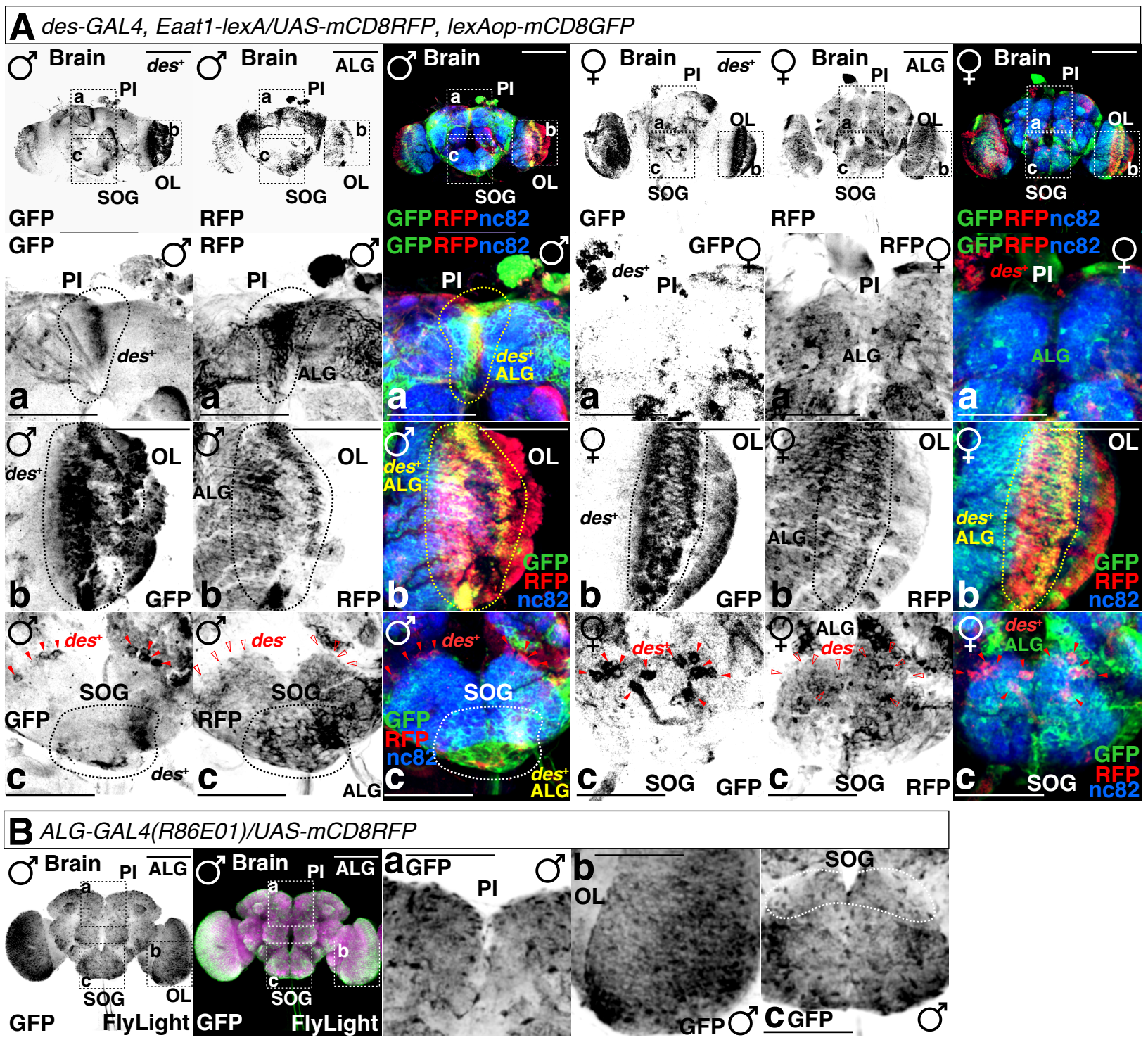
A des-GAL4, Eaat1-lexA/UAS-mCD8RFP, lexAop-mCD8GFP
Brain
des+
ALG
PI
OL
SOG
GFP
RFP
GFP RFP nc82
a
b
c
des+
ALG
GFP
RFP
nc82
B ALG-GAL4(R86E01)/UAS-mCD8RFP
FlyLight

Hadi., Fig.4

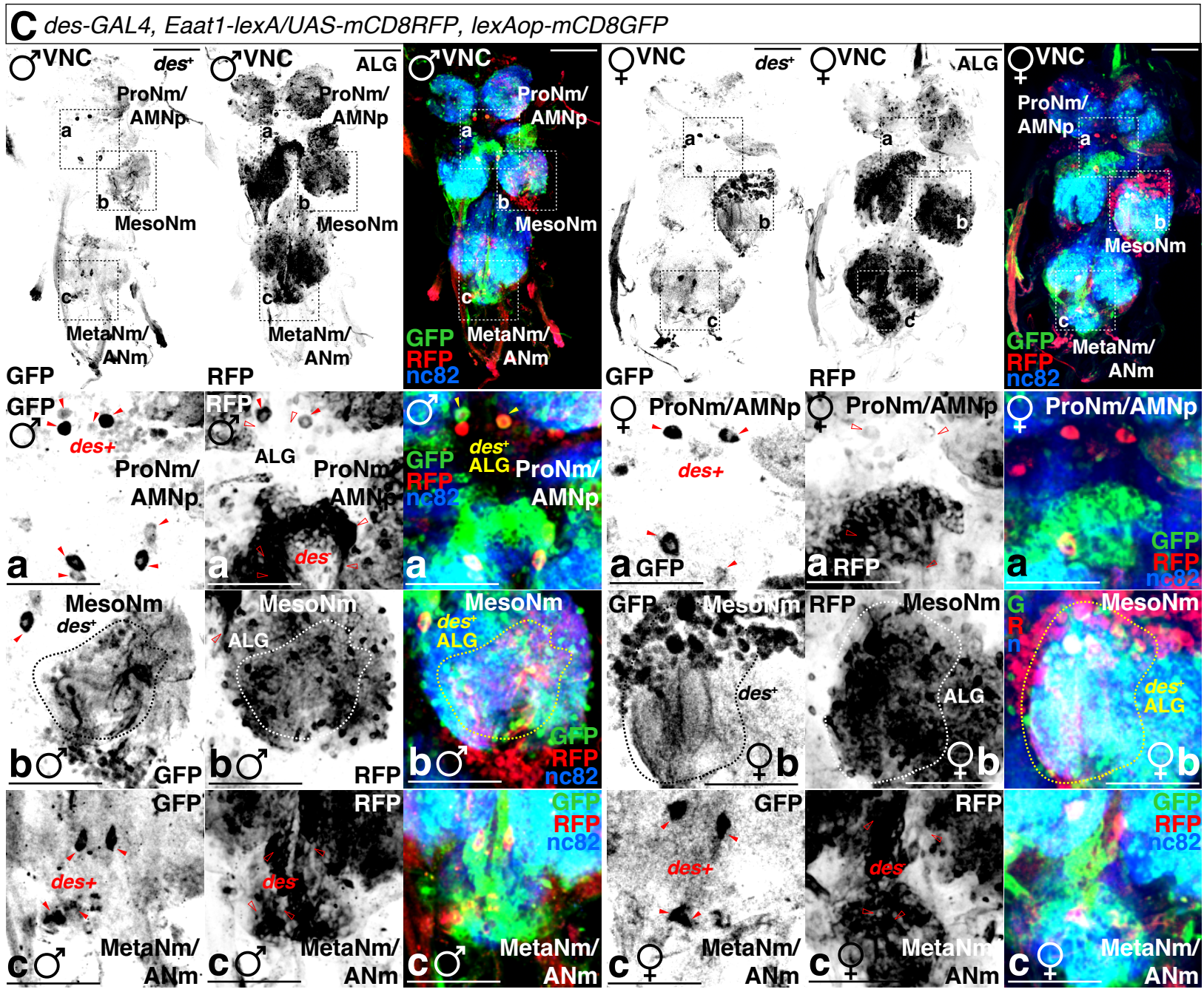
C des-GAL4, Eaat1-lexA/UAS-mCD8RFP, lexAop-mCD8GFP
♂VNC
des+
ALG
ProNm/
AMNp
MesoNm
MetaNm/
ANm
GFP
RFP
nc82
♀VNC
a
b
c
des+
des-
ProNm/AMNp
MesoNm
MetaNm/
ANm

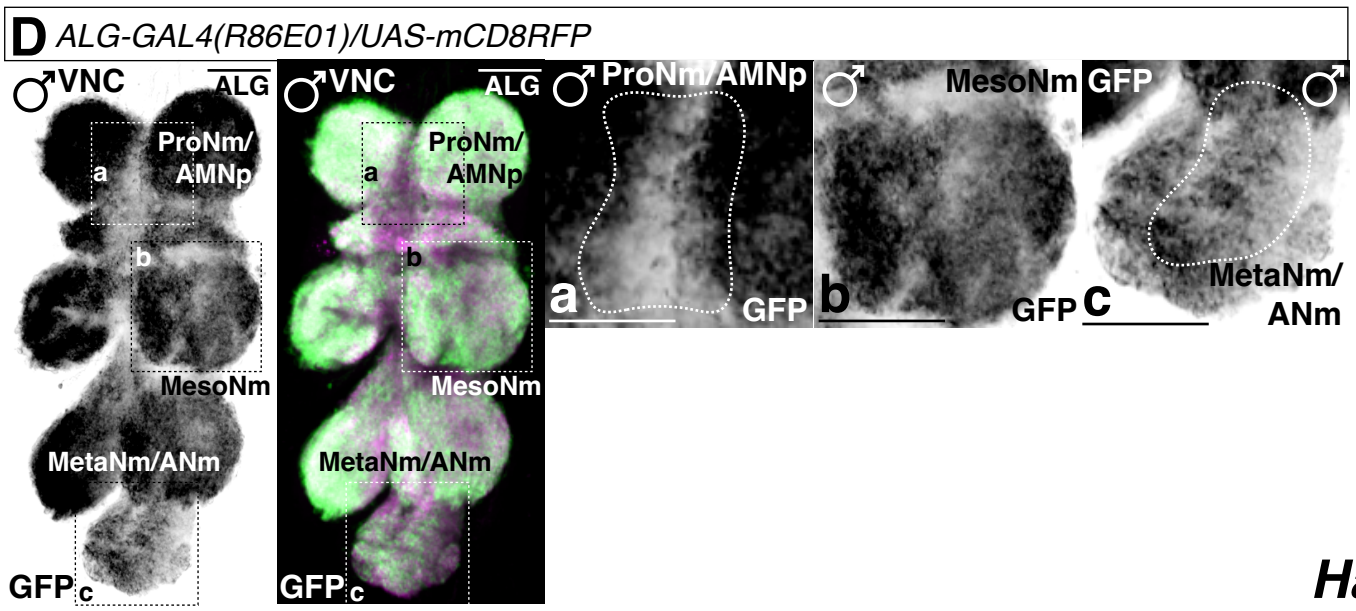
D ALG-GAL4(R86E01)/UAS-mCD8RFP
♂VNC
ALG
ProNm/
AMNp
MesoNm
MetaNm/ANm
GFP
a
b
c

Hadi., Fig.4

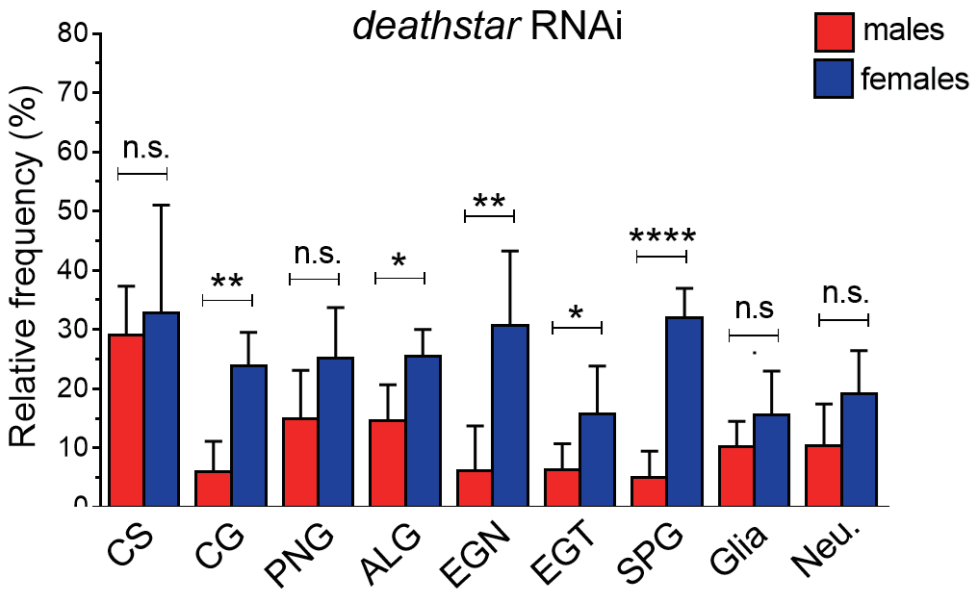
deathstar RNAi
males
females
Relative frequency (%)
0
10
20
30
40
50
60
70
80
n.s.
**
n.s.
*
**
*
****
n.s
n.s.
CS
CG
PNG
ALG
EGN
EGT
SPG
Glia
Neu.

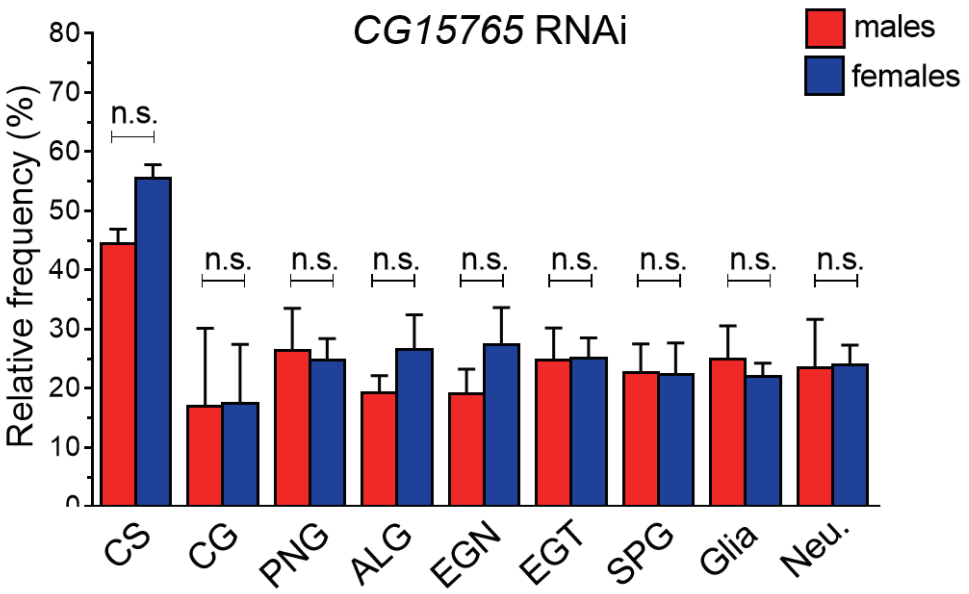
CG15765 RNAi
males
females
Relative frequency (%)
0
10
20
30
40
50
60
70
80
n.s.
n.s.
n.s.
n.s.
n.s.
n.s.
n.s.
n.s.
n.s.
CS
CG
PNG
ALG
EGN
EGT
SPG
Glia
Neu.

Hadi., Fig.5

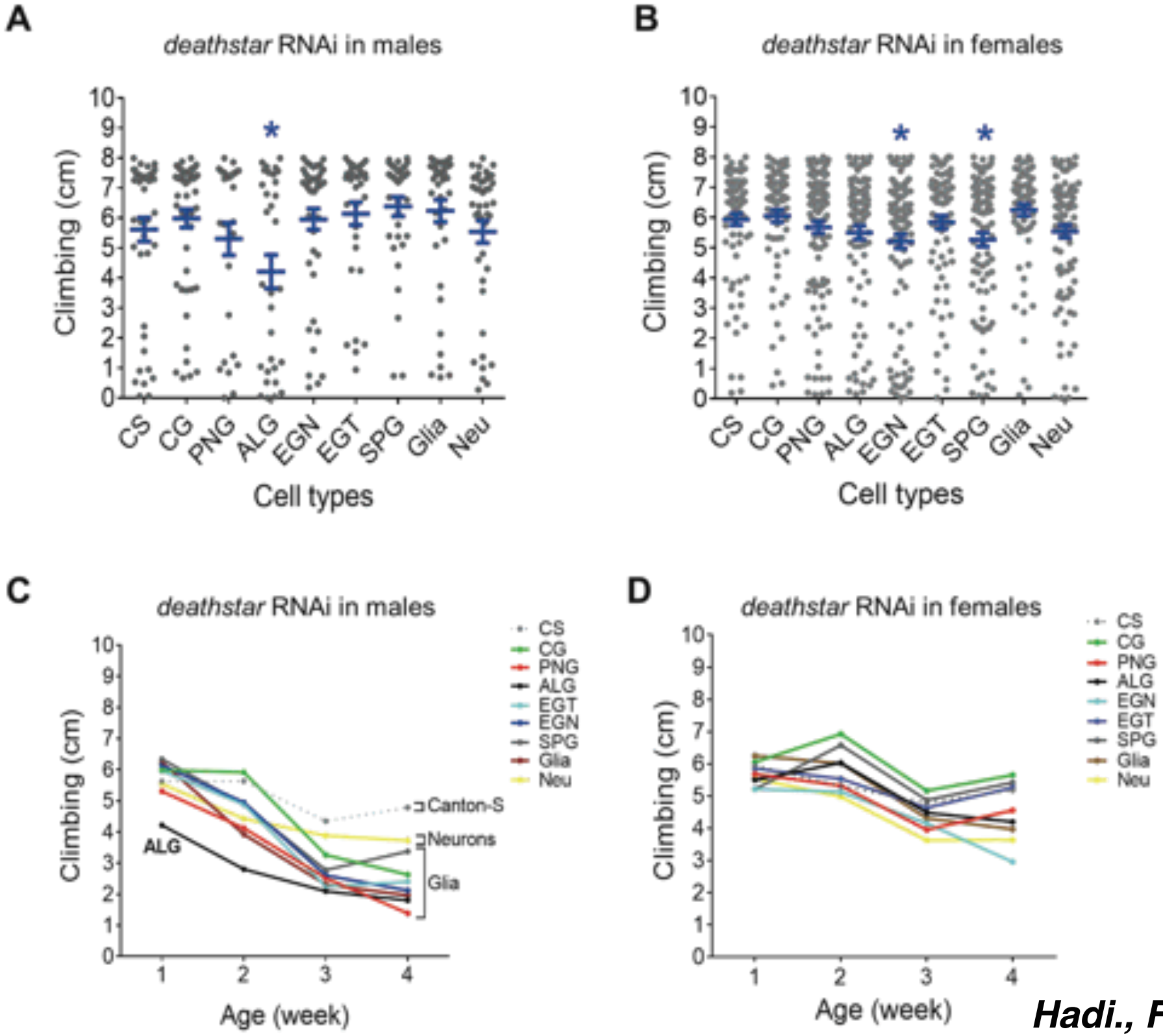
A
deathstar RNAi in males
Climbing (cm)
Cell types
CS
CG
PNG
ALG
EGN
EGT
SPG
Glia
Neu
B
deathstar RNAi in females
Climbing (cm)
Cell types
C
deathstar RNAi in males
Climbing (cm)
Age (week)
ALG
Canton-S
Neurons
Glia
D
deathstar RNAi in females
Climbing (cm)
Age (week)

Hadi., Fig.6

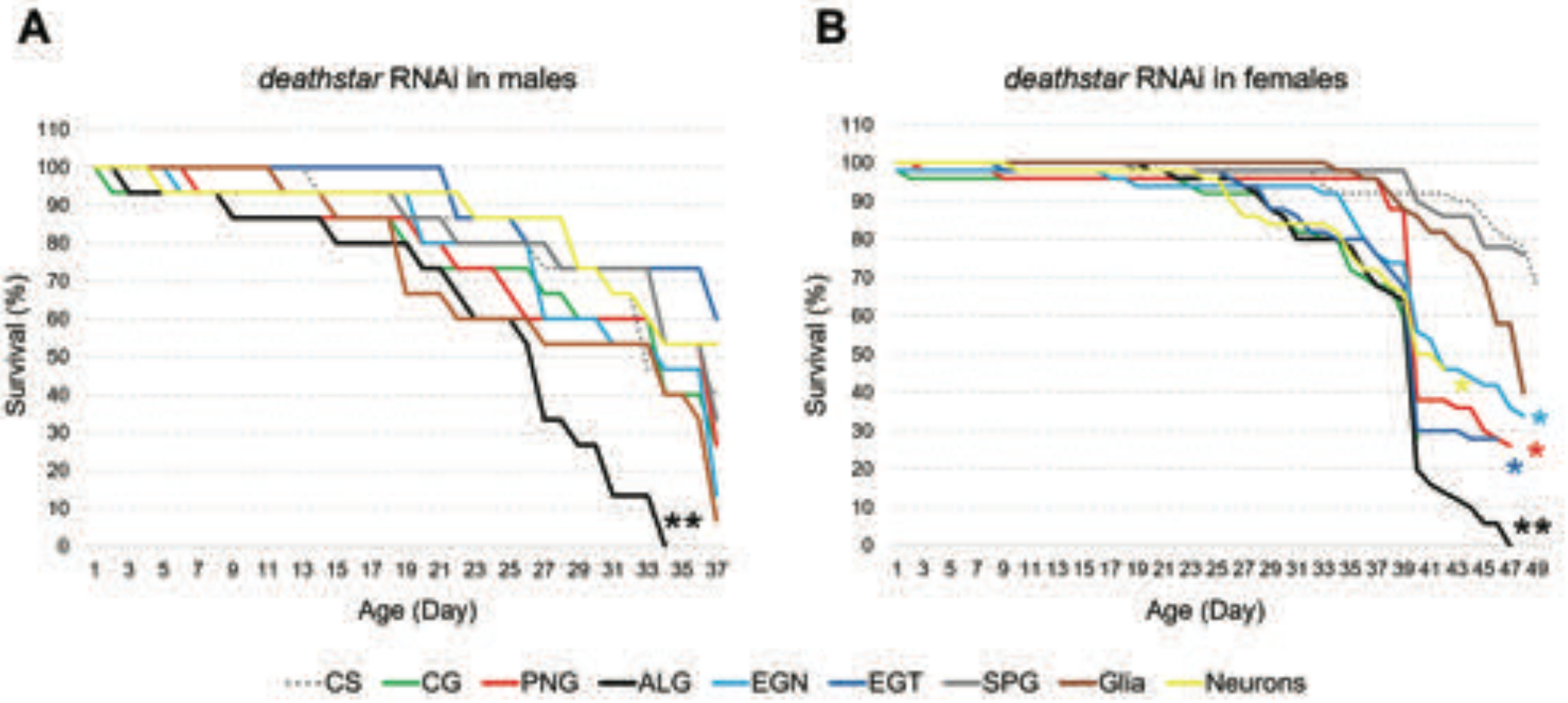
A
deathstar RNAi in males
Survival (%)
Age (Day)
B
deathstar RNAi in females
Survival (%)
Age (Day)
CS
CG
PNG
ALG
EGN
EGT
SPG
Glia
Neurons

Hadi., Fig.7

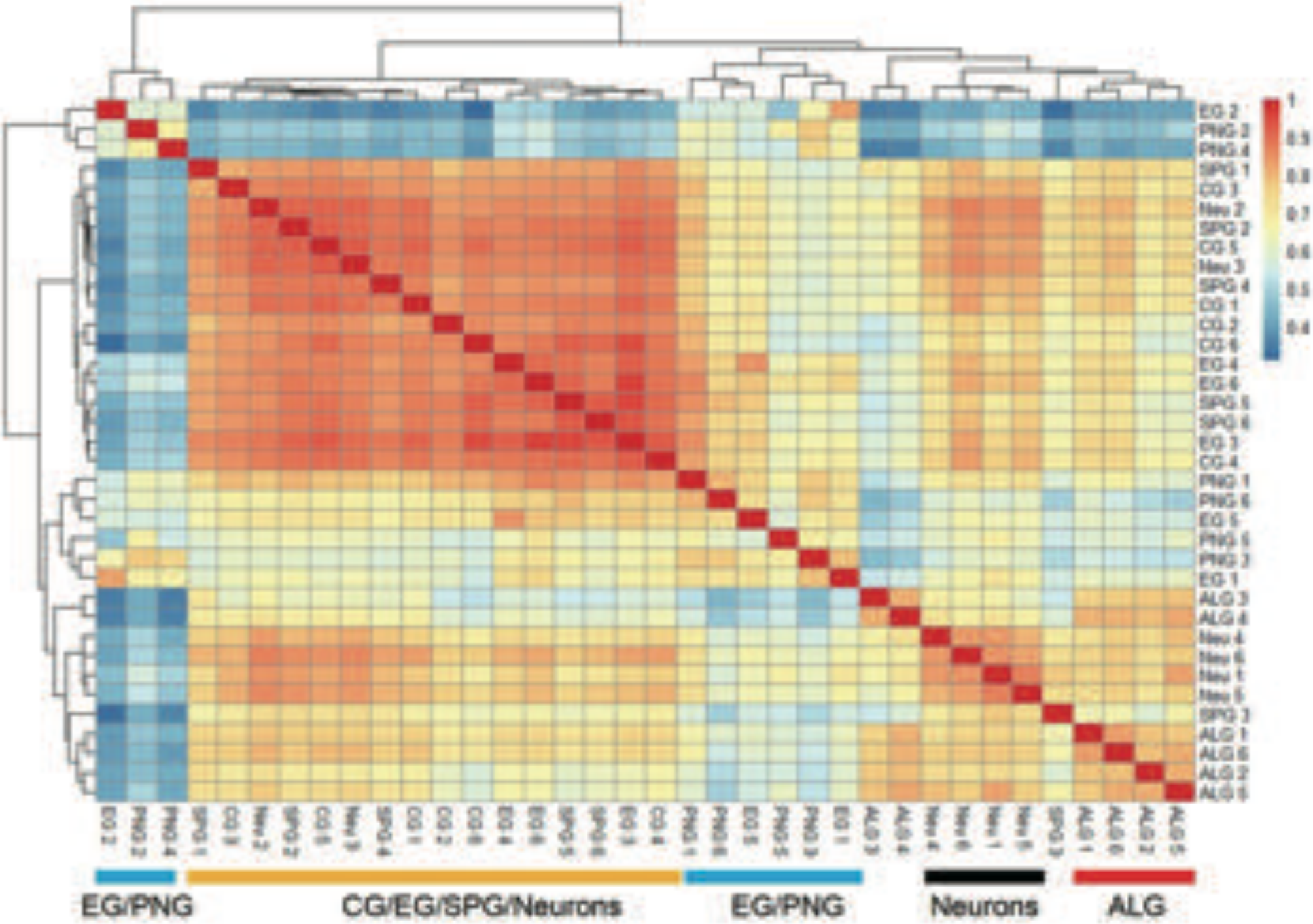

Hadi., Fig.S1

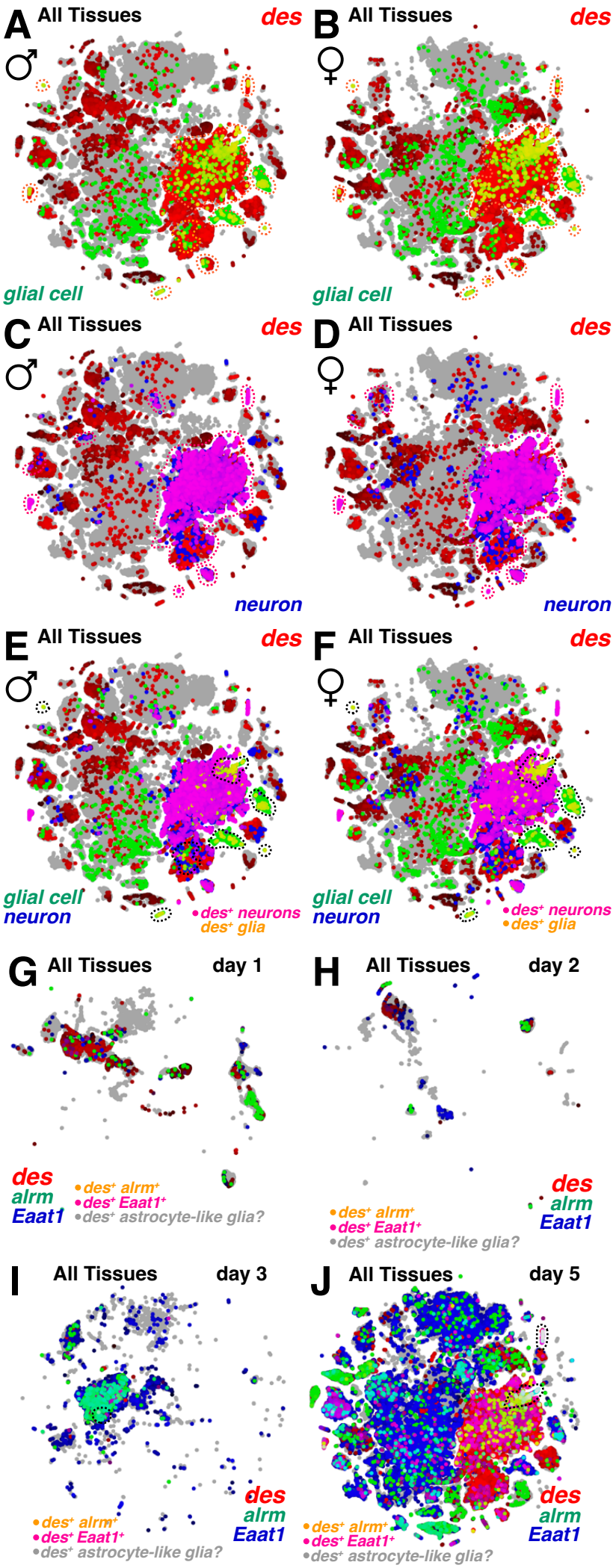
A
All Tissues
des
♂
glial cell
B
All Tissues
des
♀
glial cell
C
All Tissues
des
♂
neuron
D
All Tissues
des
♀
neuron
E
All Tissues
des
♂
glial cell
neuron
des+ neurons
des+ glia
F
All Tissues
des
♀
glial cell
neuron
des+ neurons
des+ glia
G
All Tissues
day 1
des
alrm
Eaat1
des+ alrm+
des+ Eaat1+
des+ astrocyte-like glia?
H
All Tissues
day 2
des
alrm
Eaat1
des+ alrm+
des+ Eaat1+
des+ astrocyte-like glia?
I
All Tissues
day 3
des
alrm
Eaat1
des+ alrm+
des+ Eaat1+
des+ astrocyte-like glia?
J
All Tissues
day 5
des
alrm
Eaat1
des+ alrm+
des+ Eaat1+
des+ astrocyte-like glia?

Hadi., Fig.S2

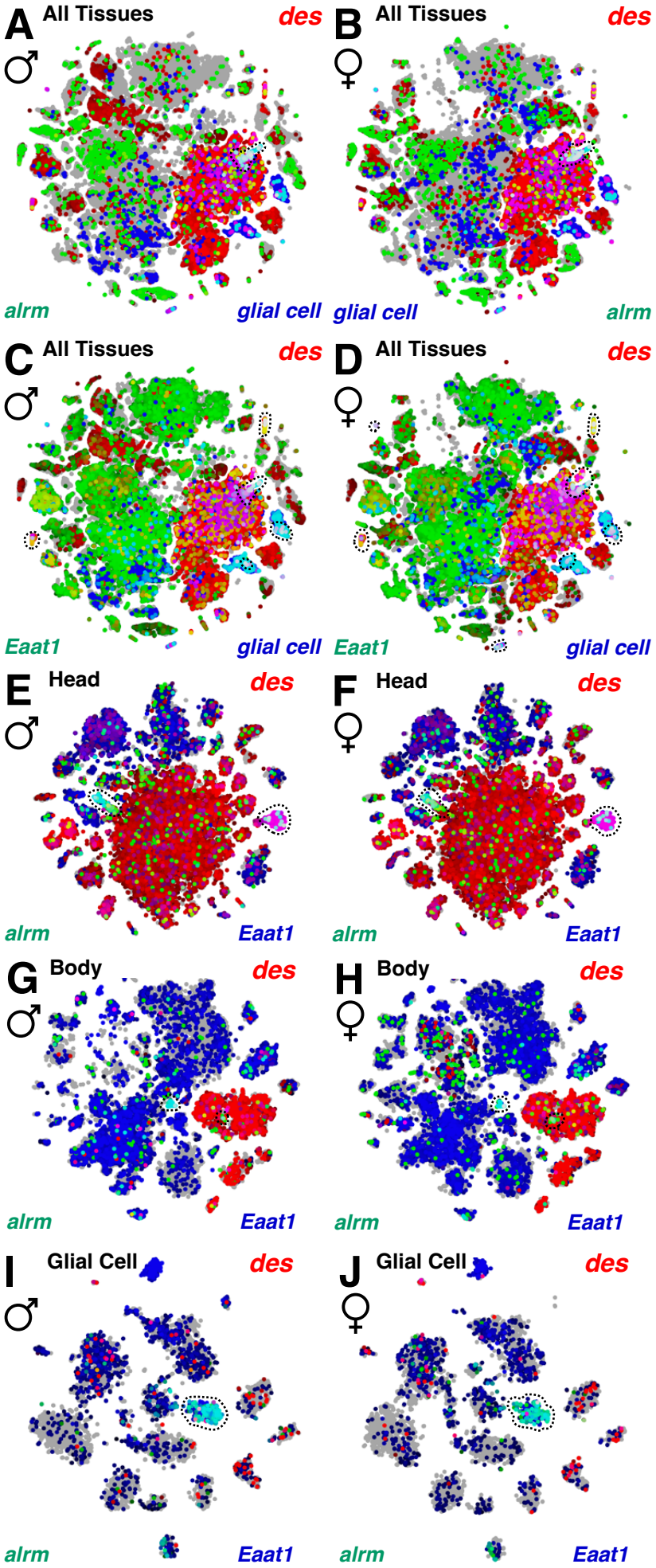
A
All Tissues
des
♂
alrm
glial cell
B
All Tissues
des
♀
glial cell
alrm
C
All Tissues
des
♂
Eaat1
glial cell
D
All Tissues
des
♀
Eaat1
glial cell
E
Head
des
♂
alrm
Eaat1
F
Head
des
♀
alrm
Eaat1
G
Body
des
♂
alrm
Eaat1
H
Body
des
♀
alrm
Eaat1
I
Glial Cell
des
♂
alrm
Eaat1
J
Glial Cell
des
♀
alrm
Eaat1

Hadi., Fig.S3

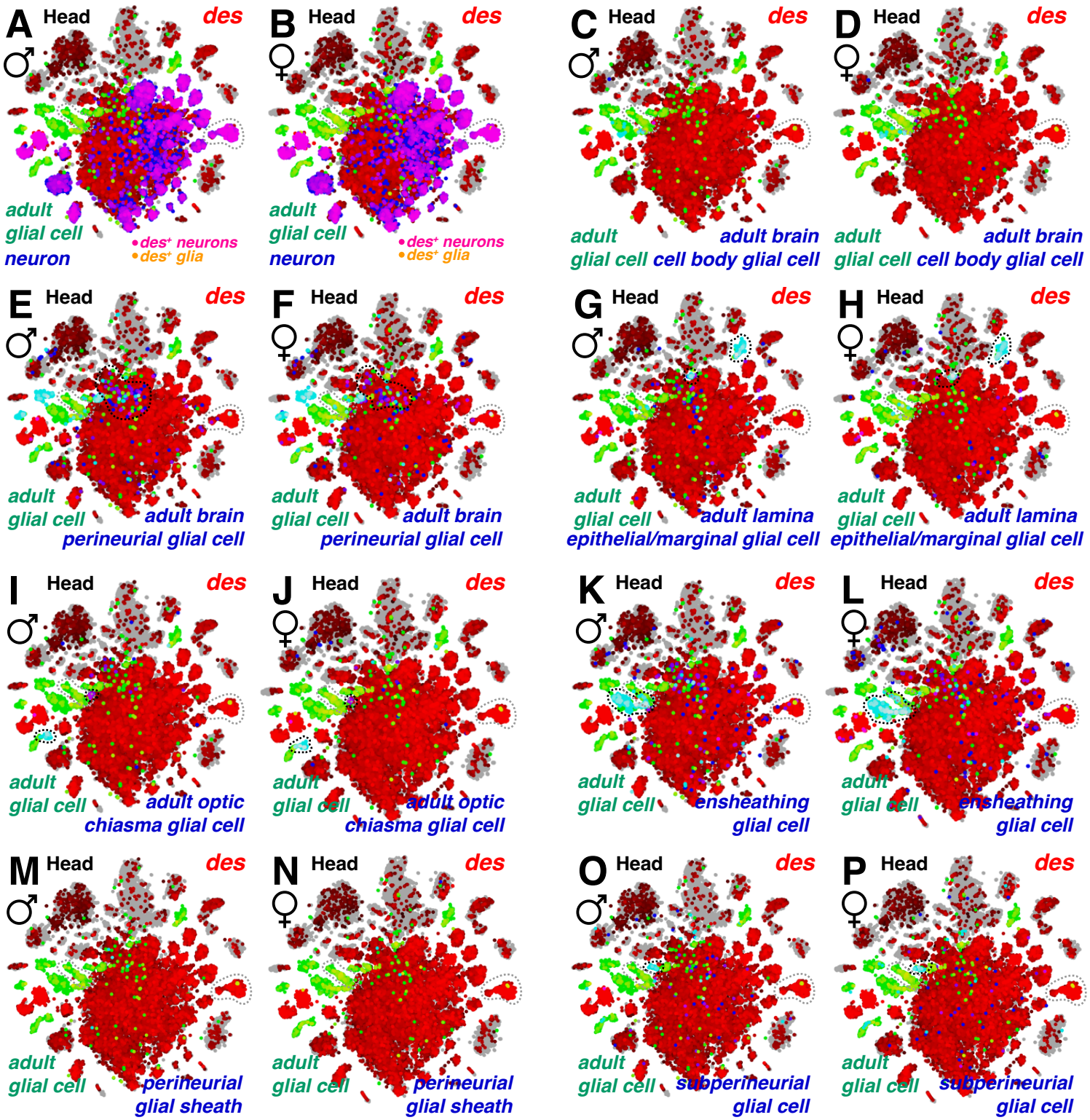
A
Head
des
♂
adult glial cell
neuron
des+ neurons
des+ glia
B
Head
des
♀
adult glial cell
neuron
des+ neurons
des+ glia
C
Head
des
♂
adult glial cell
adult brain cell body glial cell
D
Head
des
♀
adult glial cell
adult brain cell body glial cell
E
Head
des
♂
adult glial cell
adult brain perineurial glial cell
F
Head
des
♀
adult glial cell
adult brain perineurial glial cell
G
Head
des
♂
adult glial cell
adult lamina epithelial/marginal glial cell
H
Head
des
♀
adult glial cell
adult lamina epithelial/marginal glial cell
I
Head
des
♂
adult glial cell
adult optic chiasma glial cell
J
Head
des
♀
adult glial cell
adult optic chiasma glial cell
K
Head
des
♂
adult glial cell
ensheathing glial cell
L
Head
des
♀
adult glial cell
ensheathing glial cell
M
Head
des
♂
adult glial cell
perineurial glial sheath
N
Head
des
♀
adult glial cell
perineurial glial sheath
O
Head
des
♂
adult glial cell
subperineurial glial cell
P
Head
des
♀
adult glial cell
subperineurial glial cell

Hadi., Fig.S4

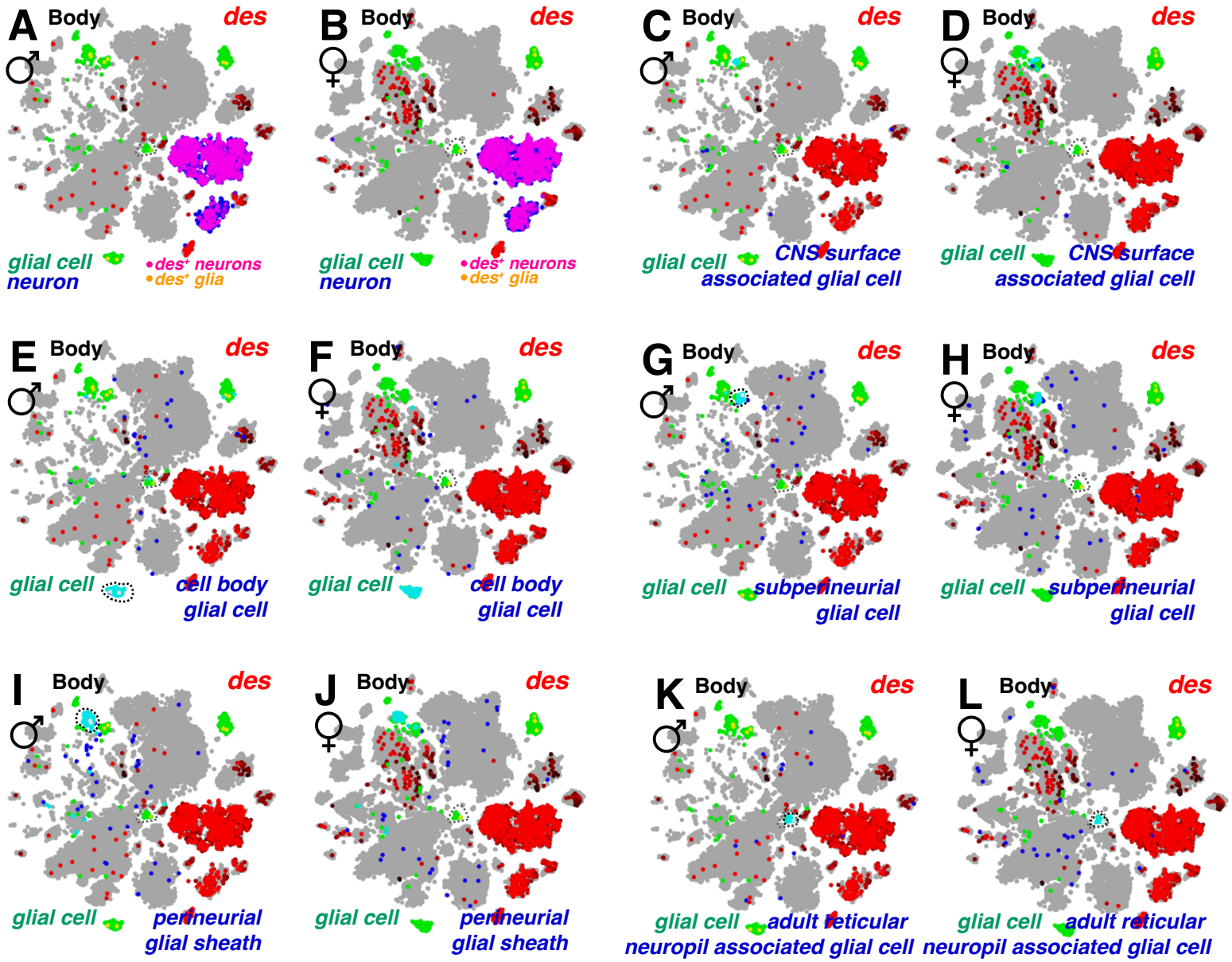
A
Body
des
♂
glial cell
neuron
des+ neurons
des+ glia
B
Body
des
♀
glial cell
neuron
des+ neurons
des+ glia
C
Body
des
♂
glial cell
CNS surface
associated glial cell
D
Body
des
♀
glial cell
CNS surface
associated glial cell
E
Body
des
♂
glial cell
cell body
glial cell
F
Body
des
♀
glial cell
cell body
glial cell
G
Body
des
♂
glial cell
subperineurial
glial cell
H
Body
des
♀
glial cell
subperineurial
glial cell
I
Body
des
♂
glial cell
perineurial
glial sheath
J
Body
des
♀
glial cell
perineurial
glial sheath
K
Body
des
♂
glial cell
adult reticular
neuropil associated glial cell
L
Body
des
♀
glial cell
adult reticular
neuropil associated glial cell

Hadi., Fig.S5

Parents for crosses		Progenies
UAS- RNAi lines (♀)	GAL4 lines (♂)	
w^+ ; +/+ ; *deathstar*-RNAi (# 51918)	wild type	wild type
w^+ ; +/+ ; *deathstar*-RNAi	+ ; +/+ ; PNG-GAL4/ TM3	Non-TM3
w^+ ; +/+ ; *deathstar*-RNAi	+ ; +/+ ; SPG-GAL4/ TM3	Non-TM3
w^+ ; +/+ ; *deathstar*-RNAi	+ ; +/+ ; CG-GAL4/ TM3	Non-TM3
w^+ ; +/+ ; *deathstar*-RNAi	+ ; +/+ ; EGN-GAL4/ TM3	Non-TM3
w^+ ; +/+ ; *deathstar*-RNAi	+ ; +/+ ; EGT-GAL4/ TM3	Non-TM3
w^+ ; +/+ ; *deathstar*-RNAi	+ ; +/+ ; ALG-GAL4/ TM6B	Non-TM6B
w^+ ; +/+ ; *deathstar*-RNAi	+ ; +/+ ; Neuron-GAL4/ TM6B	Non-TM6B

Table 1. Summary of crosses and experimental genotypes for behavioral analyses. In order to generate the transgenic flies with expression of *deathstar*-RNAi in cell type-specific manner, the male flies of different GAL4 driver lines were crossed with the females harboring UAS-*deathstar*-dsRNAi in their genome (BDSC#: 51918). All the females (♀) for these crosses were virgin. Among the progenies of these crosses, the flies with proper genotypes were selected based on the absence of balancer chromosomes (CyO, TM3 and TM6B).

Lines	Fly stocks (Genotypes and Bloomington ID)	Cross scheme
A	UAS-mCD8RFP, lexAop-mCD8GFP ; Sp/CyO ; TM2/TM6B (#32229)	P: A ♀ × B ♂ F_1: C ♂ × D ♀ F_2: E (♂ or CNS dissec
B	ALG-LexA/CyO ; TM2/TM6B (#45914)	
C	UAS-RFP, lexAop-GFP ; ALG-LexA/CyO ; TM2/TM6B	
D	*deathstar* -GAL4 (# 23416)	
E	UAS-RFP, lexAop-mCD8GFP ; ALG-LexA/+ ; TM6B/ *deathstar* -GAL4	

Table 2. Crossing scheme for imaging experiments of CNS in *Drosophila*. The line A contains RFP and GFP reporter genes under regulation of UAS and LexAop sequences, respectively. Line B expresses LexA protein in an ALG-specific manner. By crossing the lines A and B (Parents), the fly line C (F_1 generation) was produced and then crossed with *deathstar* -GAL4 line (D) to produce F_2 generation. Among the flies of F_2, the males and females that lack balancer chromosomes but contain the components of the binary systems UAS/GAL4 and LexA/LexAop were selected for central nervous system (CNS) dissection. The females (♀) of all crosses were virgin.

Supplemental Table S1. Number of newly-eclosed flies under suppression of *Deathstar* gene in neural cell types of *D. melanogaster*. The number of male progenies was less than the females when the *Deathstar* expression was suppressed in neural cell types of *D. melanogaster* (RNAi carriers). As control of the experiment, a fly line which had no expression of *Deathstar* RNAi (referred as balancer carrier) was used. Equal number of males and females was observed for this control (CS) group.

Day of collection	Fly genotypes	CS		CG		PNG		ALG		EGN		EGT		SPG		Glia		Neu.	
		♂	♀	♂	♀	♂	♀	♂	♀	♂	♀	♂	♀	♂	♀	♂	♀	♂	♀
1	RNAi carriers	7	15	2	6	4	6	4	12	7	24	1	5	1	12	7	9	12	11
	Balancer carriers	2	4	13	12	10	12	18	6	22	24	6	11	15	10	5	39	26	24
2	RNAi carriers	8	8	1	7	3	5	3	4	1	6	1	1	0	9	4	5	4	6
	Balancer carriers	2	6	7	16	4	6	4	3	4	14	5	8	5	9	8	32	8	16
3	RNAi carriers	2	1	2	10	7	5	4	5	0	15	2	5	1	10	2	4	2	4
	Balancer carriers	4	3	16	10	5	6	4	8	2	13	8	12	13	9	4	14	17	19
4	RNAi carriers	12	12	0	10	1	4	1	4	2	3	0	1	2	4	3	6	6	8
	Balancer carriers	3	7	7	12	2	3	8	2	4	1	4	2	2	8	7	6	8	10
5	RNAi carriers	18	16	6	17	4	5	10	12	3	9	1	1	6	23	2	3	12	20
	Balancer carriers	11	9	29	25	11	10	20	22	20	25	7	6	24	23	30	21	45	35
6	RNAi carriers	12	11	3	5	2	7	3	15	3	9	2	4	1	9	6	19	0	6
	Balancer carriers	5	6	6	6	5	12	15	11	30	25	5	4	10	15	14	16	7	7